P-3528

Design and Implementation of Power Converters with Boost Circuit for a Wind Induction Generator

A Project Report

Submitted By

N.PRASANNA RAJ - 0920105007

in partial fulfillment for the award of the degree
of

Master of Engineering
in
Power Electronics and Drives

DEPARTMENT OF ELECTRICAL & ELECTRONICS ENGINEERING

KUMARAGURU COLLEGE OF TECHNOLOGY
COIMBATORE – 641 049
(An Autonomous Institution Affiliated to Anna University of Technology, Coimbatore.)

ANNA UNIVERSITY OF TECHNOLOGY: COIMBATORE

April 2011

ANNA UNIVERSITY OF TECHNOLOGY: COIMBATORE

BONAFIDE CERTIFICATE

Certified that this project report entitled **"Design and Implementation of Power Converters with Boost Circuit for a Wind Induction Generator"** is the bonafide work of

N.Prasanna Raj - Register No. 0920105007

Who carried out the project work under my supervision.

Signature of the Head of the Department

.....

Dr.Rani Thottungal

Signature of the Supervisor

.....

Prof.M.Mohanraj

Assistant Professor (SRG)/EEE

Certified that the candidate with university Register No. 0920105007 was examined in project viva voce Examination held on 26/4/11

Internal Examiner

External Examiner

DEPARTMENT OF ELECTRICAL & ELECTRONICS ENGINEERING

KUMARAGURU COLLEGE OF TECHNOLOGY, COIMBATORE 641 049

(An Autonomous Institution Affiliated to Anna University of Technology, Coimbatore.)

PSNA

COLLEGE OF ENGINEERING & TECHNOLOGY

Kothandaraman Nagar, Dindigul - 624 622.

"Kalvithanthai"
Thiru. R.S.Kothandaraman
Founder

Estd : 1984

Department of Electrical & Electronics Engineering

Power Conversion, system, drives and control Technology CONference

PCTCON '11

Certificate

This is to certify that Mr / ~~Ms~~ N.Prasanna Raj of Kumaraguru College of Technology, Coimbatore has participated in the 5th National Conference on Power Conversion, system, drives and control Technology (PCTCON' 11) held on 25th February 2011 and presented a paper entitled "Design of Power Converter with Boost circuit for a Wind Induction Generator"

Secretary

Principal

Hindusthan College of Engineering and Technology

(Affiliated to Anna University of Technology,Coimbatore and Accredited by NBA,New Delhi)

Coimbatore - 641032

Department of Electrical and Electronics Engineering

Second National Conference on Control and Power Engineering

CAPECON 2011

02 March 2011

Certificate

This is to certify that Dr./Prof./Mr./Ms./ ..N.PRASANNA..RAJ..,..KUNJARAGURU..... .COLLEGE..OF..TECHNOLOGY..,..COIMBATORE.....has presented a paper titled .DESIGN....OF.....POWER....CONVERTER....WITH....BOOST...CIRCUIT...FOR..A....WIND...INDUCTION..... ...GENERATOR..... at Second National Conference on Control and Power Engineering (CAPECON 2011) held on 02 March 2011.

Organizing Secretary
Prof.M.P.VISWANATHAN

Convenor
Prof.N.P.ANANTHAMOORTHY

Principal
Dr.V.DURAISAMY

ACKNOWLEDGEMENT

I humbly submit all the glory and thanks to the almighty for showering the blessings and giving the necessary wisdom for accomplishing this project.

I would like to express my deep sense of gratitude and profound thanks to my guide **Mr.M.Mohanraj**, Assistant Professor (SRG), Electrical and Electronics Engineering Department, for his valuable guidance, support, constant encouragement and co-operation rendered throughout the project.

I take immense pleasure in thanking **Dr. Rani Thottungal**, HOD, Department of Electrical and Electronics Engineering, Kumaraguru College of Technology, for her constant encouragement and support.

I would like to express my heartfelt thanks to our beloved Principal **Dr.S.Ramachandran,** for his support.

I am also thankful to all my **teaching and supporting staff** of Electrical and Electronics Engineering department, for their kind help and encouragement.

Last but not least, I extend my sincere thanks to my **parents and friends** who have contributed their ideas and encouraged me for completing this project.

CONTENTS

ABSTRACT

This project presents the design and implementation of a power converter for an autonomous wind induction generator (IG) feeding an isolated load through the PWM-based novel soft-switching interleaved boost converter. The output voltage and frequency of the wind IG is inherently variable due to random fluctuation of wind-speed variation. The interleaved boost converter composed of two shunted elementary boost conversion units and an auxiliary inductor. This converter is able to turn on both the active power switches at zero voltage to reduce their switching losses and evidently raise the conversion efficiency. Since the two parallel-operated elementary boost units are identical, operation analysis and design for the converter module becomes quite simple. A three-phase induction machine model and a three-phase rectifier-inverter model based on a-b-c reference frame are used to simulate the performance of the generation system. It can be concluded from the simulated results that the designed power converters with adequate control scheme can effectively improve the performance of output voltage and frequency of the IG feeding an isolated load.

LIST OF FIGURES

ABBREVIATIONS

VSCF	Variable Speed Constant Frequency
SEIG	Self-Excited Induction Generator
IBC	Interleaved Boost Converter
WPU	Wind Power Unit
WEC	Wind Energy Converter
HAWT	Horizontal-Axis Wind Turbines
VAWT	Vertical-Axis Wind Turbines
CCM	Continues Current Mode
DCM	Discreet Current Mode
IGBT	Insulated Gate Bipolar Transistor
MOSFET	Metal Oxide Semiconductor Field Effect Transistor
PWM	Pulse Width Modulation
PIC	Peripheral Interface Controller
THD	Total Harmonic Distortion

CHAPTER 1

OVERVIEW OF WINDMILL POWER GENERATION

1.1 INTRODUCTION

Electric power has emerged as one of the most important elements in our daily livelihood in recent years. Power interruption leading to various outcomes has been experienced and is proven to be a threat to power consumers especially in larger industries. Renewable Energy Sources are those energy sources which are not destroyed when their energy is harnessed. The developing countries of the world, especially the ones that are resource-poor and population-rich, are confronted with a multitude of complex problems involving population growth, economics, energy, and development Unfortunately, all these problems are closely interrelated and they have been seriously aggravated by the unprecedented increases in the oil prices of the recent past. All reasonable solutions to alleviate these problems involve sharp increases both in the amount of energy consumed and in the efficiency of their use. Human use of renewable energy requires technologies that harness natural phenomena, such as sunlight, wind, waves, water flow, and biological processes such as anaerobic digestion, biological hydrogen production and geothermal heat. Amongst the above mentioned sources of energy there has been a lot of development in the technology for harnessing energy from the wind. Wind is the motion of air masses produced by the irregular heating of the earth's surface by sun. These differences consequently create forces that push air masses around for balancing the global temperature or, on a much smaller scale, the temperature between land and sea or between mountains.

1.2 PROBLEM IDENTIFICATION

In the decades to come, developing countries will certainly need more commercial fuels and will have to explore and develop all of their conventional resources to meet their growing demands from urban and suburban areas and from their industrial sectors. Renewable energy systems appear to be viable in locations where electrical grid supply has not yet reached, where commercial fuels are scarce due either to their cost or unavailability or both, and where even small amounts of energy can make a considerable impact on the living environment of local people. Introduction of renewable energy systems in rural areas must be preceded by a careful study of the technical, economic, and socioeconomic aspects of the region involved. Integrated systems can take advantage of the inherent diversity among the

different manifestations of solar energy, decouple the input and the output energy rates, and satisfy the various energy needs as and when they occur and in the form required. This project is concerned with the role of renewable energy sources. The renewable energy sources that are not very site-specific and are most prevalent in the rural areas of developing countries are solar radiation and solar heat, wind energy, falling water, and biomass (wood, agricultural wastes, human, and animal wastes).

1.3 WIND AS RENEWABLE ENERGY

The development of wind power in India began in the 1990s, and has significantly increased in the last few years. Although a relative newcomer to the wind industry compared with Denmark or the US, India has the fifth largest installed wind power capacity in the world. In 2009-10 India's growth rate is highest among the other top four countries.

Renewable sources often produce power and voltage varying with natural conditions and must be connected into the utility to be efficiently exploited. Power electronic converters are usually required for the utility interface. New technologies, materials and techniques are applied in wind power generator. Accordingly, direct-drive wind power generator system is brought forward, in which no gearbox is needed. So the oil-leak problem is avoided and no noisy eliminator need to be installed. These advantages can also reduce the insurance cost, lengthen the longevity of the generator and decrease the cost of operation and maintenance. Direct-drive variable speed constant frequency (VSCF) wind power generator system is a ideal topology. It can enable the wind turbine to run in a very wide speed range and it also leaves out the gearbox, which is used to make the rotational speed higher. The result is that the efficiency and the reliability are improved. At the same time, the maintenance cost and the direct cost are also reduced.

1.3.1 Role of Boost Circuit in Wind Power Generation

Boost converters are popularly employed in equipments for different applications. For high-power-factor requirements, boost converters are the most popular candidates, especially for applications with dc bus voltage much higher than line input. Boost converters are usually applied as preregulators or even integrated with the latter-stage circuits or rectifiers into single-stage circuits. Most renewable power sources, such as photovoltaic power systems and fuel cells, have quite low-voltage output and require series connection or a voltage booster to provide enough voltage output.

Boost converters are widely used as power-factor-corrected pre-regulators. In high power applications, interleaved operation (the parallel connection of switching converters) of two or more boost converters has been proposed to increase the output power and to reduce the output ripple. This technique consists of a phase shifting of the control signals of several cells in parallel operating at the same switching frequency. As a result, the input and output current waveforms exhibit lower ripple amplitude and smaller harmonics content than in synchronous operation modes. The resulting cancellation of low-frequency harmonics allows the reduction of size and losses of the filtering stages. However, hard switched PWM converters have low conduction losses and high switching losses. The switching losses of the boost switches create a significant amount of power dissipation in high power application.

1.4 SELF-EXCITED INDUCTION GENERATOR

The characteristics of a self-excited induction generator (SEIG) with an externally connected capacitor bank have been extensively explored for over 75 years since 1935. The primary merits of a SEIG over a conventional synchronous generator are brushless construction with squirrel-cage rotor, small size, without DC supply for excitation, less maintenance cost, and better transient performance. The SEIGs have been extensively utilized as suitable isolated power sources in small hydroelectric, tidal, and wind energy applications at the remote sites, rural areas, or developing countries.

1.5 EXISTING SCHEMES

The control schemes proposed so far divides into three categories. The most economic method is by means of switching series and/or parallel capacitors connected to the SEIG stator winding or load side for voltage regulation. The primary disadvantage of this scheme is that the equivalent capacitance is changed in discrete form and the voltage cannot be effectively and linearly regulated. Though the voltage magnitude is controlled to a certain constant level, the output frequency of the controlled SEIG is significantly varied with the rotor speed. The second method is to modulate the absorbed reactive power of the studied SEIG whose stator windings is directly connected to the load and the reactive power compensator. Although the terminal voltage of the stator winding can be effectively controlled, the frequency variation problem due to random fluctuation of rotor speed is similar to the one of the first method. The third method is the most effective control scheme, which can control both voltage and frequency of the studied SEIG within a specified level by

using power electronic converters such as a rectifier-inverter module (AC-to-DC and DC-to-AC converters). The employed rectifier can be either a controlled converter or an uncontrolled diode bridge rectifier. A SEIG fed to a local three-phase load through a diode bridge and a PWM inverter with a open/closed loop PWM signal controller was presented.

A SEIG fed to an isolated load through the employment of a PWM based open loop controlled inverter is presented. The simulated performance of the proposed control scheme is employed to design a PI controller (to generate PWM signal) for the inverter. The implementation and design of a power converter for an autonomous wind self-excited induction generator (SEIG) feeding an isolated load through the PWM-based rectifier-inverter circuit is simulated here.

1.6 OBJECTIVE OF THE PROJECT

In this project, the wind energy conversion system is proposed and deeply discussed which has many promotions compared with traditional AC-DC-AC converter. It has synchronous generator, multiple boost converter and dual three-phase PWM inverter, all the devices are designed to limit harmonic and high purity sinewave current to the network. The direct drive and robust low speed rotor design system results in minimum wear, reduces noise levels, improves efficiency, reduced maintenance requirements, lower life cycle costs, and a long life time.

Wind energy is not a constant source of energy. It varies continuously and gives energy in sudden bursts. Wind strengths vary and thus cannot guarantee continuous power. The design and implementation of a power converter for an autonomous three phase wind induction generator (IG) feeding an isolated load through the PWM-based rectifier-inverter circuit is designed here. A three-phase constant-voltage constant-frequency voltage source is required to supply an isolated load via a designed power converter with pulse width modulation (PWM). The utilizes a three-phase asynchronous machine model and a three-phase rectifier-inverter model based on a-b-c reference frame to simulate the performance of the studied generation system. The IG design is made with the calculated value of resistance, flux linkage of the stator and rotor windings and with the torque equation and the no. of poles. The terminal voltage of the SEIG model for rotor speed about 1500rpm is tested and found varying from 320V to 325V. The power converter converts the three phase AC to DC and then the filter circuit is used for obtaining smooth DC voltage across it. The inverter is designed with PWM technique to maintain the voltage and frequency constant to feed the AC

load. PWD signal is generated in open loop with PI controller. Thus the inverter part is made to operate as an open loop circuit. The voltage and the frequency at the output terminal are stabilized.

1.7 ORGANISATION OF THE REPORT

This report presents an Interleaved Boost Converter as a DC – DC converter with active power filter function .Chapter 1 gives an overview of scope of wind power generation and the importance of boost circuit in renewable energy power resource with its advantages and features. Chapter 2 deals the windmill power generation system and the existing method with its MATLAB Simulation model. Chapter 3 describes the proposed design and analysis of IBC system along with the control strategies of PWM pulses for the Boost Converter switches. The MATLAB Simulation model of the IBC system is also obtained. Chapter 4 deals with the proposed model of IBC with wind power gerneration system. It is discussed theoretically and with the MATLAB Simulation of the proposed system with the output waveforms. Chapter 5 deals with the hardware modelling of the proposed system, results of hardware testing and the process coding of the PIC controller. Chapter 6 winds up the report with the conclusion and future scope of the project.

CHAPTER 2
WIND MILL POWER GENERATION

2.1 WIND ENERGY

With the lack of energy resource, wind energy generating systems have gained tremendous attention and developed rapidly in recent years. About 50% of the entire energy is given out in just 15% of the operating time. Wind strengths vary and thus cannot guarantee continuous power. It is best used in the context of a system that has significant reserve capacity such as hydro, or reserve load, or a desalination plant, to mitigate the economic effects of resource variability. It has been demonstrated to be both technically and economically viable. It is expected that current developments in gearless, variable speed generators with power electronics grid interface will lead to a new generation of quiet, efficient, economical wind turbines. For best aerodynamic efficiency, the shaft speed should be varied in proportion to wind speed.

2.2 WIND TURBINES

A wind turbine is a rotating machine which converts the kinetic energy in wind into mechanical energy. If the mechanical energy is then converted to electricity, the machine is called a wind generator, wind turbine, wind power unit (WPU), wind energy converter (WEC), or aero-generator. Wind turbines can be separated into two types based by the axis in which the turbine rotates. Turbines that rotate around a horizontal axis are more common. Vertical-axis turbines are less frequently used.

2.2.1 Horizontal Axis Wind Turbines

Horizontal-axis wind turbines (HAWT) have the main rotor shaft and electrical generator at the top of a tower, and must be pointed into the wind. Most have a gearbox, which turns the slow rotation of the blades into a quicker rotation that is more suitable to drive an electrical generator.

Since a tower produces turbulence behind it, the turbine is usually pointed upwind of the tower. Turbine blades are made stiff to prevent the blades from being pushed into the tower by high winds. Additionally, the blades are placed a considerable distance in front of the tower and are sometimes tilted up a small amount.

Downwind machines have been built, despite the problem of turbulence, because they don't need an additional mechanism for keeping them in line with the wind, and because in high winds the blades can be allowed to bend which reduces their swept area and thus their wind resistance. Since cyclic (that is repetitive) turbulence may lead to fatigue failures most HAWTs are upwind machines.

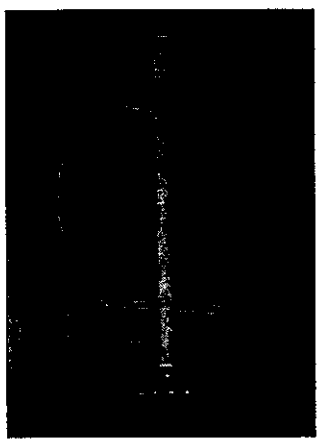

Figure 2.1 Horizontal axis wind turbine

2.2.2 Vertical axis Wind Turbines

Vertical-axis wind turbines (VAWT) have the main rotor shaft arranged vertically. Key advantages of this arrangement are that the turbine does not need to be pointed into the wind to be effective. This is an advantage on sites where the wind direction is highly variable. VAWTs can utilize winds from varying directions.

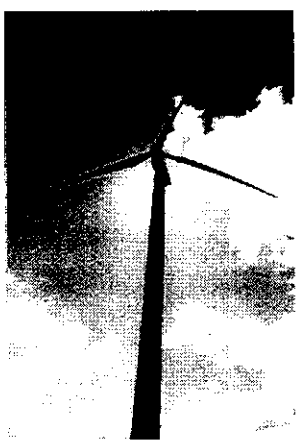

Figure 2.2 Vertical axis wind turbine

With a vertical axis, the generator and gearbox can be placed near the ground, so the tower doesn't need to support it, and it is more accessible for maintenance. Drawbacks are that some designs produce pulsating torque. Drag may be created when the blade rotates into the wind.

The following figure 2.3 deals with the parts of a wind turbine

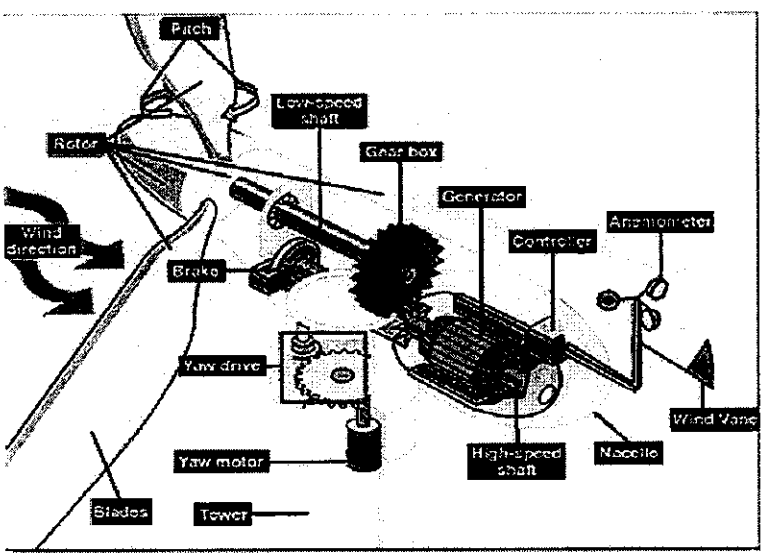

Figure 2.3 Parts of a Wind turbine

2.3 WIND TURBINE GLOSSARY

Anemometer: Measures the wind speed and transmits wind speed data to the controller.

Blades: Most turbines have either two or three blades. Wind blowing over the blades causes the blades to "lift" and rotate.

Brake: A disc brake which can be applied mechanically, electrically, or hydraulically to stop the rotor in emergencies.

Controller: The controller starts up the machine at wind speeds of about 8 to 16 miles per hour (mph) and shuts off the machine at about 65 mph. Turbines cannot operate at wind speeds above about 65 mph because their generators could overheat.

Gear box: Gears connect the low-speed shaft to the high-speed shaft and increase the rotational speeds from about 30 to 60 rotations per minute (rpm) to about 1200 to 1500 rpm, the rotational speed required by most generators to produce electricity. The gear box is a

costly (and heavy) part of the wind turbine and engineers are exploring "direct-drive" generators that operate at lower rotational speeds and don't need gear boxes.

Generator: Usually an off-the-shelf induction generator that produces 60-cycle AC electricity.

High-speed shaft: Drives the generator. Low-speed shaft: The rotor turns the low-speed shaft at about 30 to 60 rotations per minute.

Nacelle: The rotor attaches to the nacelle, which sits atop the tower and includes the gear box, low- and high-speed shafts, generator, controller, and brake. A cover protects the components inside the nacelle. Some nacelles are large enough for a technician to stand inside while working.

Pitch: Blades are turned, or pitched, out of the wind to keep the rotor from turning in winds that are too high or too low to produce electricity.

Rotor: The blades and the hub together are called the rotor.

Tower: Towers are made from tubular steel (shown here) or steel lattice. Because wind speed increases with height, taller towers enable turbines to capture more energy and generate more electricity.

Wind direction: This is an "upwind" turbine, so-called because it operates facing into the wind. Other turbines are designed to run "downwind", facing away from the wind.

Wind vane: Measures wind direction and communicates with the yaw drive to orient the turbine properly with respect to the wind.

Yaw drive: Upwind turbines face into the wind; the yaw drive is used to keep the rotor facing into the wind as the wind direction changes. Downwind turbines don't require a yaw drive, the wind blows the rotor downwind.

Yaw motor: Powers the yaw drive.

2.4 EXISTING SYSTEM

The complete configuration of the existing wind power generation system using a SEIG is shown in Figure. 2.4. The stator winding terminals of the studied SEIG are connected to the load through the rectifier, DC link, and a controlled PWM inverter. The open loop

PWM signal generates proper PWM signals to switch, 6 IGBT's of the inverter. The wind turbine rotates the IG. The IG generates power when the speed of the turbine is above the rated speed. The power generated from the IG is converted to DC with a diode bridge rectifier. The obtained DC voltage will not be in a pure DC signal. A LC filter is used to filter out the ripple current and a pure DC voltage is obtained. This DC voltage is then converted to three phase AC signal with IGBT. To regulate the AC output voltage the IGBT's are controlled by PWM signals. A load is connected at the output of the inverter.

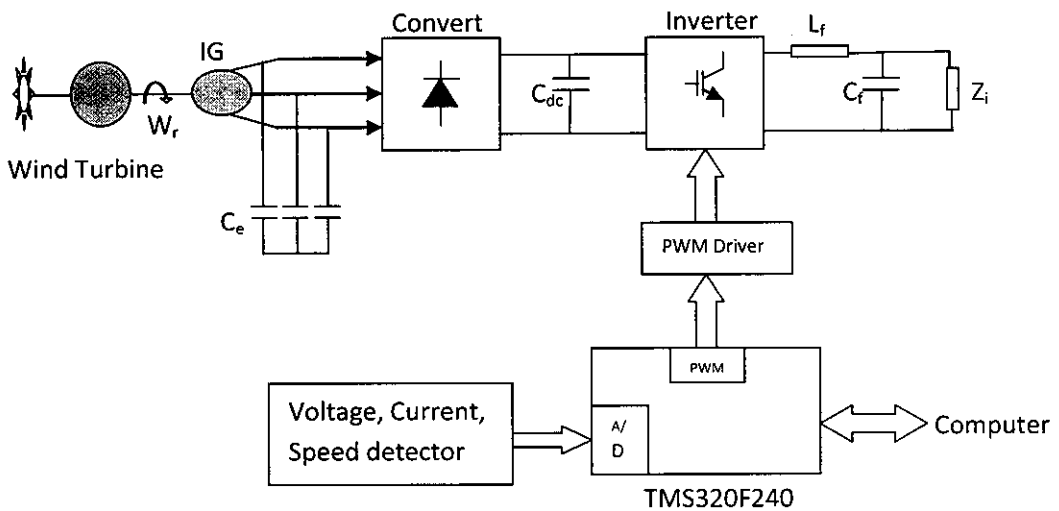

Figure. 2.4 Hardware Block Diagram

2.4.1 Design of SEIG System

The voltage-current equations of the studied SEIG in matrix form are listed as below.

$$\mathbf{v}_{s(abc)} = \mathbf{R}_{s(abc)}\mathbf{i}_{s(abc)} + p\boldsymbol{\lambda}_{s(abc)}$$
$$\mathbf{v'}_{r(abc)} = \mathbf{R'}_{r(abc)}\mathbf{i'}_{r(abc)} + p\boldsymbol{\lambda'}_{r(abc)}$$

Where Rs(abc) and R'r(abc) are respectively the resistance matrices of the stator and rotor windings and λs(abc) and λ'r(abc) are respectively the flux-linkage matrices of the stator and rotor windings [15].

Figure 2.5 shows the three-phase equivalent circuit model for the studied SEIG system represented in stator and rotor parameters. The employed differential equations of the studied SEIG system from excitation capacitors, bridge rectifier, DC link, and inverter are extensively derived in detail. The mechanical torque equations of the studied SEIG are given The mechanical torque equations of the studied SEIG are given as below.

$$2Hp(\omega_r) = T_m - T_e$$
$$p(\theta_r) = \omega_r$$

Where H is the inertia, Tm is the input mechanical torque,

The electrical torque, Te can be expressed by

$$T_e = (\frac{N_p}{2})[i_{s(abc)}]^T \frac{\partial}{\partial \theta_r} [L'_{sr}][i'_{r(abc)}]$$

Where Np is the number of pole of the studied SEIG.

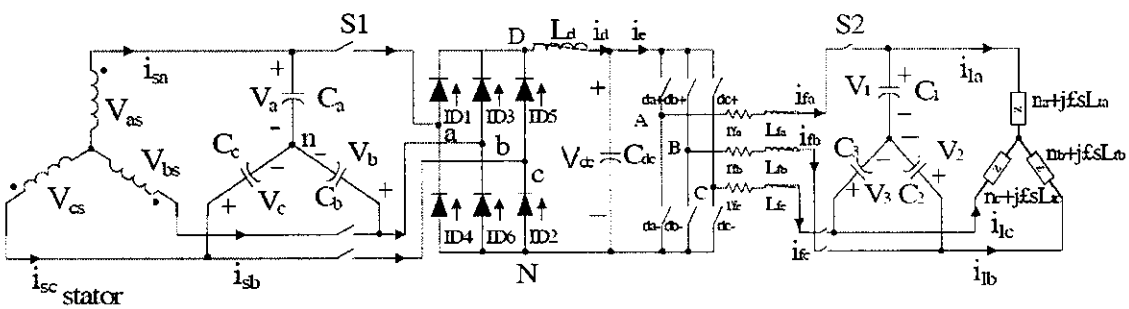

Figure 2.5 Three phase equivalent circuit of SEIG system

The power extracted from the wind can be calculated by the given formula:

$$P_W=0.5\rho\pi R^3 Vw^3 C_P(\lambda,\beta)$$

P_w = extracted power from the wind,

ρ = air density, (approximately 1.2 kg/m^3 at 20°C at sea level)

R = blade radius (in m), (it varies between 40-60 m)

V_w= wind velocity (m/s) (velocity can be controlled between 3 to 30 m/s)

C_p = the power coefficient which is a function of both tip speed ratio (λ), and blade pitch angle, (β)(deg.)

Power coefficient (Cp) is defined as the ratio of the output power produced to the power available in the wind. No wind turbine could convert more than 59.3% of the kinetic energy of the wind into mechanical energy turning a rotor. This is known as the Betz Limit, and is the theoretical maximum coefficient of power for any wind turbine. The maximum value of C_P according to Betz limit is 59.3%. For good turbines it is in the range of 35-45%.

The tip speed ratio (λ) for wind turbines is the ratio between the rotational speed of the tip of a blade and the actual velocity of the wind. High efficiency 3-blade-turbines have tip speed ratios of 6–7. For a giving wind turbine, as the two parameters ρ and A are constants, the value of the output power depends on the performance coefficient Cp and the wind speed. To maximize this output power, and as the wind speed is varying from time to

time, the performance coefficient must be maximized. Therefore, it must be controlled. Its expression is

$$C_p(\lambda,\beta) = C_1\left(\frac{C_2}{\lambda_i} - C_3\beta - C_4\right)\exp\left(-\frac{C_5}{\lambda_i}\right) + C_6\lambda$$

2.4.2 Mathematical model

The per-phase equivalent circuit of a three-phase short-shunt induction generator with its excitation capacitors and an R-L load is shown in Figure 2.6, where R1, X1, R2, X2, Rc and Xm represent the stator resistance, stator leakage reactance, rotor resistance, rotor

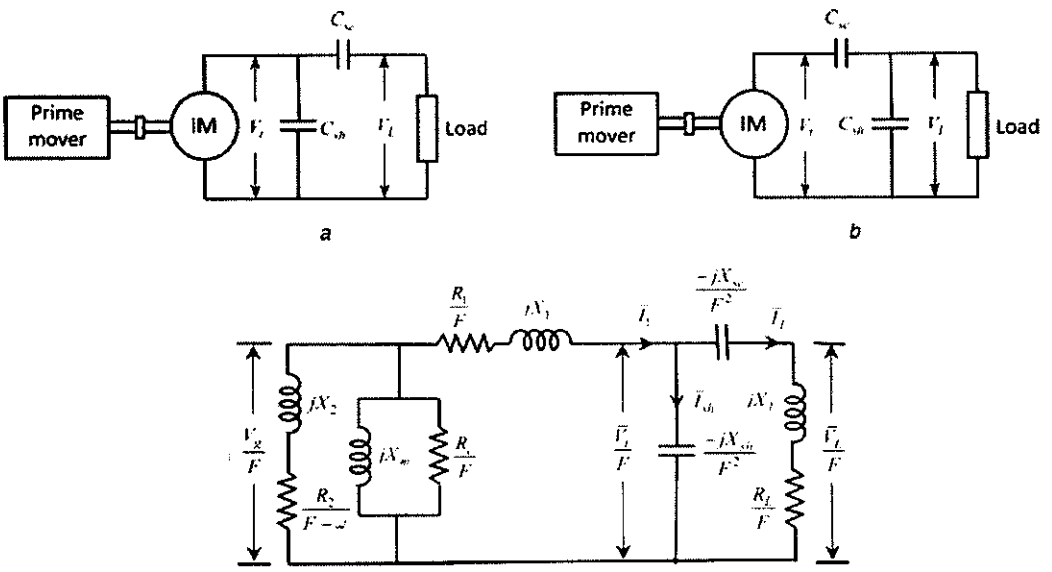

Figure 2.6 Per-phase equivalent circuit of a three-phase short-shunt induction generator

leakage reactance, core loss resistance and magnetising reactance, respectively. F and v represent the per unit (pu) frequency and speed, respectively. The reactance of the series and shunt capacitors is represented by Xse and Xsh, respectively. The load impedance is represented by ZL/u ¼ (RL þ jXL). The pu frequency F and the pu speed v are defined as

$$F = \frac{f}{f_b} \quad \text{and} \quad \omega = \frac{N}{N_s}$$

Here, f and N are the actual operating frequency (Hz) and rotor speed (rpm), respectively, of the generator, and fb and Ns are the base or rated frequency (Hz) and the corresponding synchronous speed (rpm), respectively, of the machine. When the generator operates at a frequency other than the base frequency, all reactances (inductive and capacitive) are to be adjusted accordingly. In a generic way, the inductive reactances are to be multiplied by the pu

frequency F and the capacitive reactances are to be divided by F. The circuit shown in Figure 2.6 represents a generic equivalent circuit of the generator where all parameters (resistances and reactances) and voltages are divided by the pu frequency F, whereas the currents remain the same. The above circuit is used in for both fixed and variable speed operations of the generator. All parameters of the generator, except the magnetising reactance, are considered as constant. The variation of magnetising reactance Xm is the main factor in the process of the voltage build-up and stabilisation of the operating point of an SEIG. The value of Xm depends on magnetic saturation or air-gap flux, which in turn depends on the ratio of the air-gap voltage to frequency (Vg/F). The relationship between Vg/F and Xm can be established from the synchronous speed test results. Mathematically, the above relationship can be expressed in many ways such as a linear function, piecewise linear function, an exponential function or a higher-order polynomial. In this study, Vg/F is expressed by the following third-order polynomial of Xm

$$\frac{V_g}{F} = k_0 + k_1 X_m + k_2 X_m^2 + k_3 X_m^3$$

Induction generators are widely used in nonconventional power generation. Self-excited, squirrel cage induction generators are ideally suited for remote, stand-alone applications due to their robust construction. A new closed loop IGBT based PWM controller is proposed for self-excited induction generator. The proposed controller regulates the excitation current of the induction generator to regulate the generated three phase voltage. The terminal voltage is regulated in spite of varying rotor speed and different load conditions. The proposed scheme does not require any real time computation for generating reference currents. This low cost high performance controller is suitable for constant voltage variable frequency loads. The digital simulation results show satisfactory operation of induction generator under proposed control scheme.

2.4.3 Simulation Model of Existing System

The designed system generates AC power with a asynchronous generator (215HP; 400V; 50Hz). The generated is rectified, filtered for a pure DC voltage. This DC signal voltage is made as regulated AC three phase with IGBT's. A PWM signal is generated to regulate the AC voltage at the output. Thus a regulated Three Phase AC supply is transmitted

to the Load. Figure 2.8 shows the simulation diagram of the existing wind power generation system.

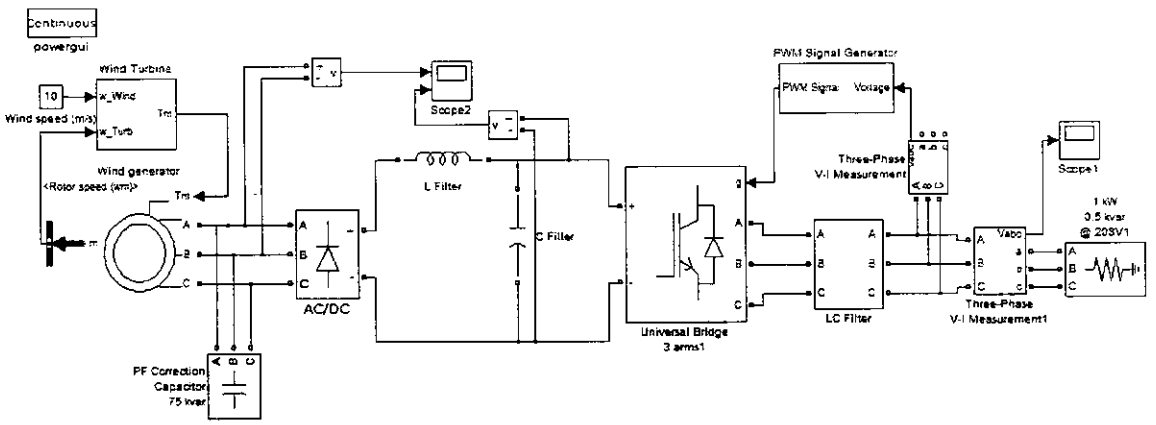

Figure 2.7 Simulation Diagram of existing wind generation system

2.4.4 Drawbacks of Existing System

- Power rating of the wind generator should be high.
- Wind speed required for required power generation is high.
- Gear mechanism between wind turbine and the generator is complex.
- Harmonic content in the power generated is high.
- Control of inverter part is bit complex as it needs to generate PWM signal with the reference obtained from the AC. The AC voltage needs to be converted to DC for setting reference voltage.

CHAPTER 3

INTERLEAVED BOOST CONVERTER

3.1 BOOST CIRCUIT

Boost converters are popularly employed in equipments for different applications. For high-power-factor requirements, boost converters are the most popular candidates, especially for applications with dc bus voltage much higher than line input. Boost converters are usually applied as preregulators or even integrated with the latter-stage circuits or rectifiers into single-stage circuits. Most renewable power sources, such as photovoltaic power systems and fuel cells, have quite low-voltage output and require series connection or a voltage booster to provide enough voltage output.

3.2 INTERLEAVED BOOST CIRCUIT

Converters with interleaved operation are fascinating techniques nowadays. Interleaved boost converters are applied as power-factor-correction front ends. An interleaved converter with a coupled winding is proposed to provide a lossless clamp. Additional active switches are also appended to provide soft-switching characteristics. These converters are able to provide higher output power and lower output ripple. This paper proposes a soft-switching interleaved boost converter composed of two shunted elementary boost conversion units and an auxiliary inductor. This converter is able to turn on both the active power switches at zero voltage to reduce their switching losses and evidently raise the conversion efficiency. Since the two parallel-operated boost units are identical, operation analysis and design for the converter module becomes quite simple. In laboratory, a test circuit is built to provide a 500 W power output. The experimental results show that this converter module performs very well with the output efficiency as high as 95%.

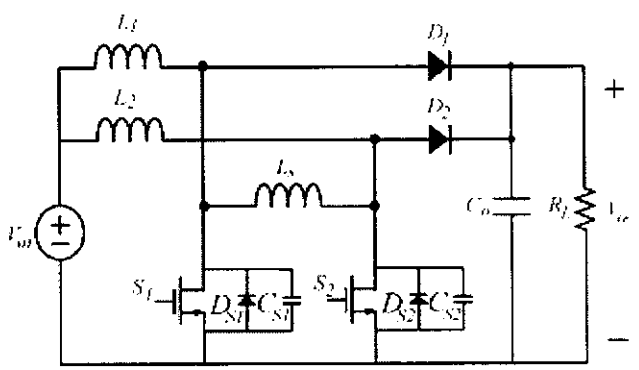

Figure 3.1 Interleaved Boost Converter

There are several common techniques that have been used for dc/dc converter control, such as voltage mode control, peak current mode control and average current mode current. The current mode control is preferred because it can achieve a faster transient response when a power demand is requested by the upper level command. To choose between peak current mode control and average current mode control, average current mode is preferred with the consideration of the normal operating mode of the converter. It is known that controlling the inductor average current in current mode control regulates the output voltage of the converter. In CCM mode, peak current mode control presents exact average inductor current due to the continuity of the inductor current. While in DCM operation, the inductor average current cannot be represented by the inductor peak current individually. Since the converter is designed to work under CCM/DCM boundary condition only at full load, the dual loop average current mode control is a better solution. In the dual loop structure, the outer loop is voltage loop, which provides the current reference for the inner current loop. This control requires the sampling of three variables: output voltage *Vbus*, inductor current *IL1* and *IL2*, which are obtained through conventional Hall transducers.

There are in general two basic approaches in designing digital controller. The first is to transform the controlled plant model to the discrete time domain and then use direct digital control design method such as root locus to design the controller. The drawback of this method is that it lacks of the common control concept such as crossover frequency and phase margin that can be applied in the design stage. The second approach favoured by practicing engineers is to design the controller in continuous time domain first so that enough information about crossover frequency and phase margin are available, and then convert the controller from continuous time domain to discrete time domain. To guarantee the stability of the design, the zero-order-hold effect and the computational delay have to be included in the controller design in the continuous time domain. In this paper the second approach is Adopted to design the dual-loop regulator.

3.3 IBC OPERATION

Figure.3.2 shows the proposed soft-switching converter module. Inductor L1, MOSFET active switch S1 and diode D1 comprise one step-up conversion unit, while the components with subscript "2" form the other. Dsx and Csx are the intrinsic antiparallel diode and output capacitance of MOSFET Sx, respectively. The voltage source Vin, via the

two paralleled converters, replenishes output capacitor C0 and the load. Inductor Ls is shunted with the two active MOSFET switches to release the electric charge stored within the output capacitor C_{sx} prior to the turn-ON of S_x to fulfill zero-voltage turn- ON (ZVS), and therefore, raises the converter efficiency. To simplify the analysis, L1, L2 and C0 are replaced by current and voltage sources, respectively, as shown in Figure 3.3. The proposed circuit is focused on higher power demand applications. The inductors L1 and L2 are likely to operate under continuous conduction mode (CCM); therefore, the peak inductor current can be alleviated along with less conduction losses on active switches. Under CCM operation, the inductances of L1 and L2 are related only to the current ripple specification. Inductance of L_s is the one which dominates the output power range and ZVS operation.

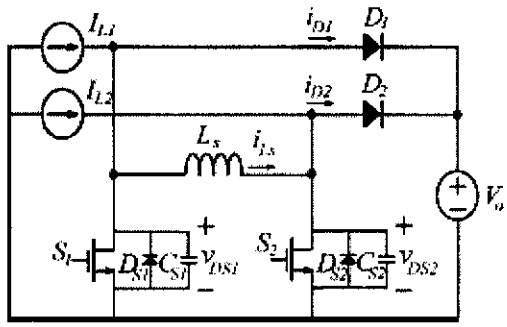

Figure 3.2 IBC simplified circuit

Before analysis on the circuit, the following assumptions are presumed.

- The output capacitor is large enough to reasonably neglect the output voltage ripple.
- The forward voltage drops on MOSFET and diodes and is neglected.
- Inductors and have large inductance, and their currents are identical constants, i.e.
- Output capacitances of switches and have the same values, i.e.

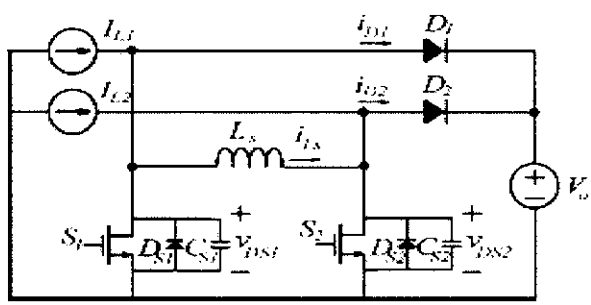

Figure 3.3 IBC Study

The two active switches are operated with pulse width-modulation (PWM) control signals. They are gated with identical frequencies and duty ratios. The rising edges of the two gating signals are separated apart for half a switching cycle. The operation of the converter can be divided into eight modes, and the equivalent circuits are illustrated in Figure 3.4

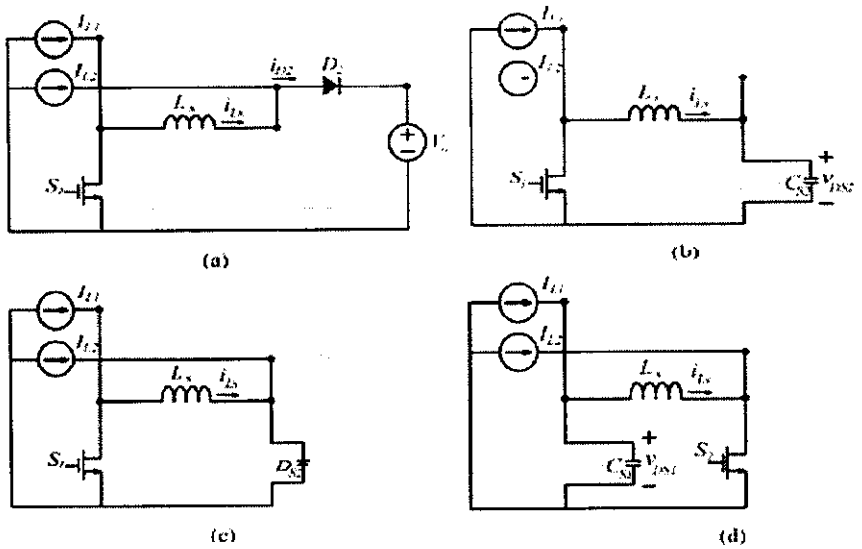

Figure 3.4 IBC Operation

• Mode I $\{t_0 < t < t_1\}$

Prior to this mode(referring to Figure 3.4(a)), the gating signal for switch S_2 has already transmitted to low state and the voltage V_{DS2} rises to V_0 at t_0 . At the beginning of this mode, current flowing through S_2 completely commutates to D_2 supply the load. Current i_{S1} returns from negative value toward zero; I_{L1} flows through L_s . Due to the zero voltage on v_{DS1} , the voltage across inductor L_s is V_o, i.e., i_{Ls} will decrease linearly at the rate of V_o/L_s. Meanwhile, the current flowing through S_1 ramps up linearly. As i_{Ls} drops to zero, i_{S1} current contains only I_{L1}, while i_{D2} equals I_{L2} Current i_{Ls} will reverse its direction and flow through S_1 together with I_{L1} . As i_{Ls} increases in negative direction, i_{D2} consistently reduces to zero. At this instant, i_{Ls} equals $-I_{L2}$, diode D_2 turns OFF, and thus this mode comes to an end. Despite the minor deviation of i_{S1} from zero and i_{lls} from I_{L1}, currents i_{Ls},i_{S1},i_{D2} and the duration of this mode t_{01} can be approximated as

$$i_{Ls}(t) = I_L - \frac{V_o}{L_S}t$$

$$i_{S1}(t) = \frac{V_o}{L_S}t$$

$$i_{D2}(t) = 2I_L - \frac{V_o}{L_S}t$$

$$t_{01} = \left(\frac{3}{4} - D_{eff}\right)T_S - \frac{\sin^{-1}(V_o/(V_o + 2I_L/\omega C_S))}{\omega}$$

where D_{eff} is the effective duty ratio and $w = 1/\sqrt{LsCs}$.

• Mode II $\{t_1 < t < t_2\}$

With this mode (referring to Figure 3.4.(b)), diode D_2 stops conducting, capacitor C_{S2} is not clamped at V_0 anymore. The current flowing through Ls and i_{Ls} continues increasing and commences to discharge C_{S2}. This mode will terminate as voltage across switch S_2,v_{DS2} drops to zero. Voltage v_{DS2} and i_{Ls2} current can be equated as

$$v_{DS2}(t) = V_o \cos(\omega t)$$
$$i_{Ls}(t) = -V_o \omega C_S \sin(\omega t) - I_L$$
$$t_{12} = \frac{\pi}{2w}.$$

• Mode III $\{t_1 < t < t_3\}$

At $t=t_2$ (referring to Figure 3.4.(c)), voltage v_{DS2} decreases to zero. After this instant D_{S2}, the antiparallel diode of S_2, begins to conduct current. The negative directional inductor current i_{Ls} freewheels through S_1 and D_{S2}, and holds at a magnitude that equals i_{Ls}, a little higher than I_L. During this mode, the voltage on switch S_2 is clamped to zero, and it is adequate to gate S_2 at zero-voltage turn- ON

$$t_{23} = \left(D_{eff} - \frac{1}{2}\right) T_S.$$

• Mode IV $\{t_3 < t < t_4\}$

At $t=t_3$ (referring to Figure 3.4 (d)), the switch S_1 turns OFF. Current i_{Ls} begins to charge the capacitor C_{S1}. The charging current includes I_{L1} and i_{Ls}. Since the capacitor C_{S1} retrieves a little electric charge, i_{Ls} decreases a little and resonates toward - I_{L2}. In fact, i_{Ls} will not equal - I_{L2} at t_4 even with a slightly higher magnitude. However, by ignoring the little discrepancy, the voltage on switch S_1 and current through L_S can be approximated as

$$v_{DS1}(t) = \left(V_0 + \frac{2I_L}{\omega C_S}\right) \sin(\omega t)$$
$$i_{Ls}(t) = I_L - (V_o \omega C_S + 2I_L) \cos(\omega t)$$
$$t_{34} = \frac{\sin^{-1}(V_o/(V_o + 2I_L/\omega C_S))}{w}.$$

While the capacitor voltage v_{DS1} ramps to V_0, D_1 will be forward-biased, and thus this mode will come to an end. Modes I–IV describes the scenario of switch between OFF-state

proceeding to ZVS turn-ON. Operations from modes V–VIII are similar to the previous modes but with the counterparts for switch, hence they are omitted here.

3.4 IBC CONTROL DESIGN

3.4.1 PI controller with current limiter

Figure 3.5 shows the control loop block diagram in continuous time domain. The inner current loop controller has a transfer function of *Hi*(s), and the output loop controller has a transfer function of *Hv*(s). A current limiter is added to the output of the voltage compensation to prevent the gain from saturation.

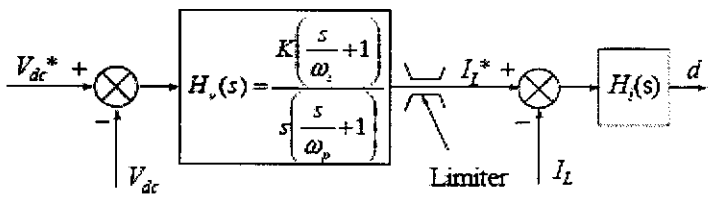

Figure 3.5 Control Loop Block Diagram in Continuous time Domain

As there is no limiter directly applied to the output of the integrator, this controller configuration can be viewed as the conventional one without anti wind-up scheme. The continuous time domain input and output relationship of the compensator is

$$U(s) = K\frac{s/\omega_z + 1}{s(s/\omega_p + 1)}I(s)$$

Where, $U(s)$ is the compensator output and $I(s)$ is compensator input. By the Euler transformation $s = T/(z - 1)$, which is a common practice for conversion from continuous time domain to discrete time domain, the following discrete time domain input and output relationship of the compensator can be obtained

$$U(k+1) = A_0U(k) + A_1U(k-1) + B_0I(k+1) + B_1I(k)$$

where $U(k)$ is compensator output at time $t = kT$, and $I(k)$ is compensator input in the discrete domain, the Constants A_0,A_1,B_0,B_1 can be given as

$$A_1 = -\frac{1}{1+\omega_p T}, \quad A_0 = \frac{2+\omega_p T}{1+\omega_p T}, \quad B_1 = -\frac{K\omega_p}{\omega_z}\frac{T}{1+\omega_p T}, \quad B_0 = \frac{K\omega_p}{\omega_z}\frac{T+\omega_z T^2}{1+\omega_p T}$$

3.5 SIMULATION DIAGRAM

The simulation block diagram of IBC is shown in Figure 3.5. IBC is parallel combination of two boost circuit connection. The simulation is tested for different input

voltage. Figure 3.6 shows the control part for the switches in IBC. The switching is controlled by PWM signals with reference voltage set to 240V. Figure 3.7 shows the input and output voltage level of IBC.

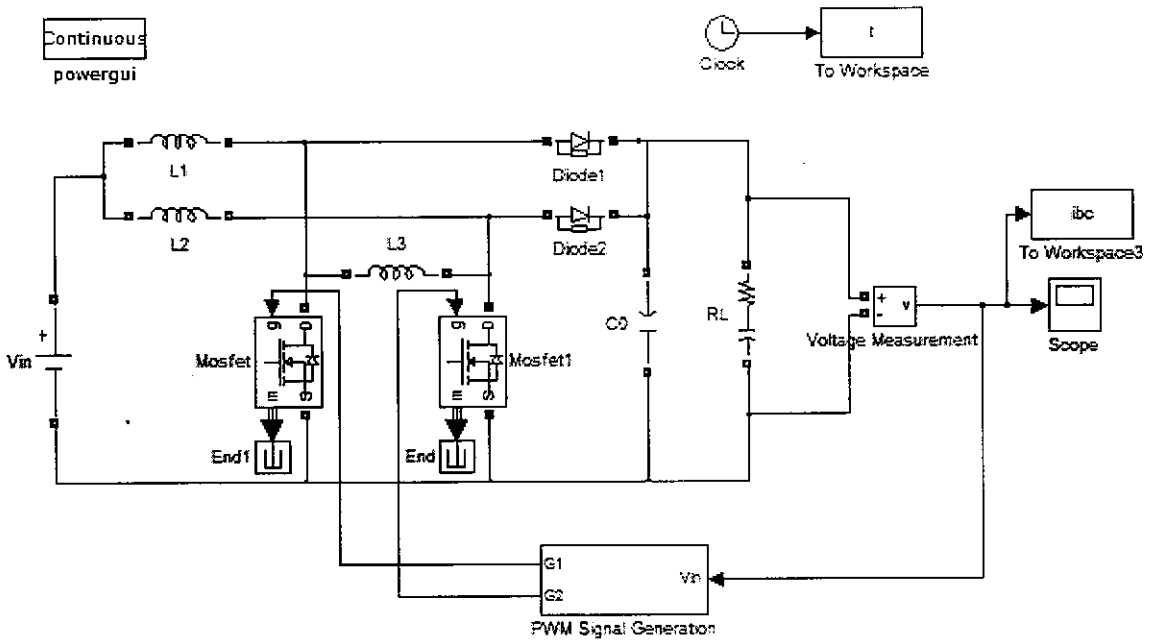

Figure 3.5 Simulation circuit of IBC

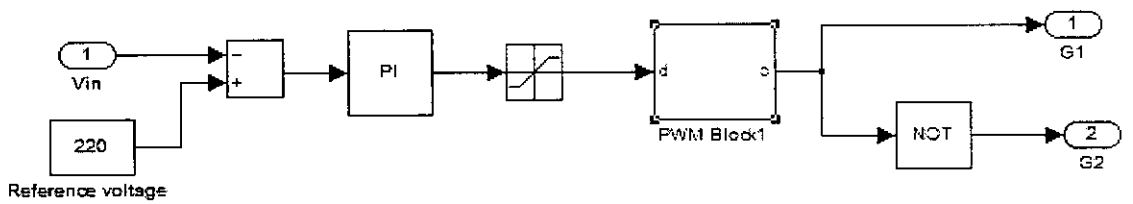

Figure 3.6 PWM Signal generation for IBC

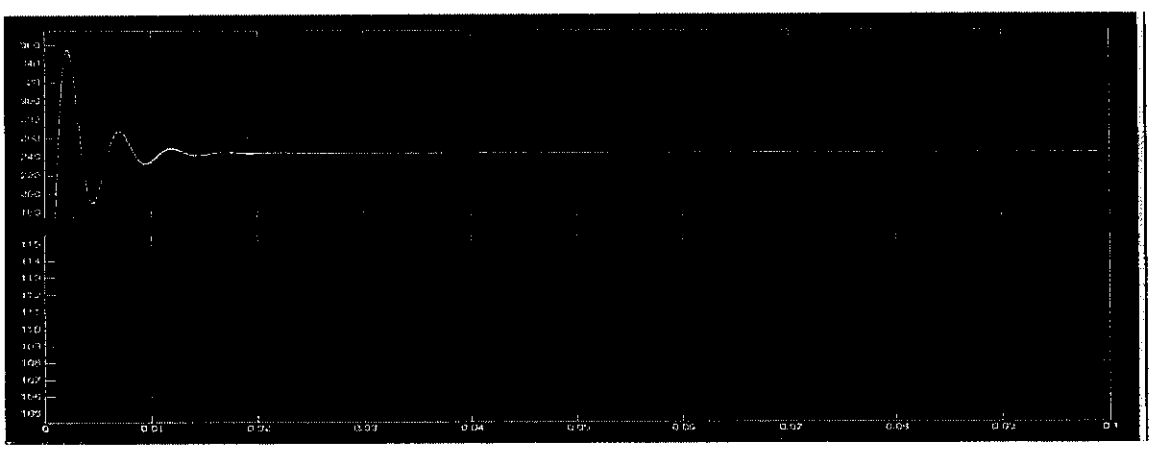

Figure 3.7 IBC – Input & Output Voltage

CHAPTER 4

DESIGN OF BOOST CONVERTER IN WIND INDUCTION GENERATOR

4.1 WIND INDUCTION GENERATOR

AC power generated by wind induction generator is rectified to DC power by 6-phase diode rectifier circuit. Following the generator, constituted a 6-phase diode rectifier circuit, filter, multiple boost converter and dual three-phase PWM inverter. The PWM converter used as the inverter applies 6 IGBT bridge modules whose modulation signal is shifted 0.8 for each phase in order to reduce harmonic distortion.

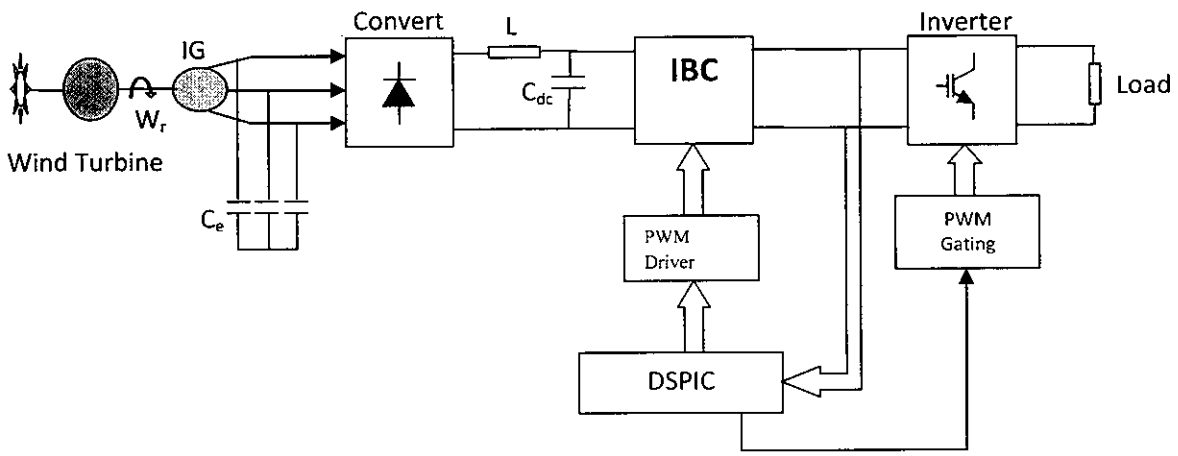

Figure 4.1 Block Diagram of wind power generator

Figure 4.1 shows the block diagram of the wind power generator system with boost circuit. It has a Self Excited Induction Generator, which generates power based on the wind speed, connected to diode rectifier. The Induction generator has excitation capacitor (C_e), which supplies voltage to the rotor. The diode rectifier is connected to IBC and then to inverter. The inverter voltage is given to the load.

The power generated by the wind induction generator will vary based on the wind speed. The minimum wind speed requires for power generation is 8m/s. Greater the wind speed higher the voltage generated by the WIG. The modified system mainly concentrated on low wind speed power generation and to obtain the required voltage level. The generated power for the current wind speed is rectified using diode rectifier. The rectified DC voltage is filtered with LC circuit. The DC voltage at the rectifier is same as the power generated at the WIG. When the wind speed decreased the power generated will also decrease. As a result the

rectified voltage level will reduce. This reduced voltage level (Wind speed<8m/s) cannot meet the required voltage at the load terminal. The project focus on boosting the voltage even when the winds speed and the generated voltage is low. The boosting operation is made with DC-DC Interleaved Boost Converter (IBC). IBC boost the voltage and regulates the voltage at the desired level. The boost voltage is stabilized by using a closed loop PWM technique, which gives the constant required DC level. The output of IBC is given to six pulse thyristor inverter. The gating signal of the thyristor is fed from the constant open loop PWM signal generator. The inverted three phase AC supply is given to the load. Thus the voltage is regulated at the load terminal.

4.2 SELECTION OF BOOST POWER STAGE COMPONENTS

The interleaved boost converter design involves the selection of the inductors, the input and output capacitors, the power switches and the output diodes. Both the inductors and diodes should be identical in both channels of an interleaved design. In order to select these components, it is necessary to know the duty cycle range and peak currents. Since the output power is channeled through two power paths, a good starting point is to design the power path components using half the output power. Basically, the design starts with a single boost converter operating at half the power. However, a trade-off exists which will depend on the goals of the design.

Knowing the maximum and minimum input voltages, the output voltage, the voltage drops across the output diode and switch, the maximum and minimum duty cycles are calculated. Next, the average inductor current can be estimated from the load current and duty cycle. Assuming the peak to peak inductor current ripple to be a certain percentage of the average inductor current, the peak inductor current can be estimated. The inductor value is then calculated using the ripple current, switching frequency, input voltage, and duty cycle information. Finally, the boundary between CCM and DCM is determined which will determine the minimum load current.

Once the inductor value has been chosen and the peak currents have been calculated, the other components may be selected. Selection of the input and output capacitors differ from a single phase design because of the reduced ripple and increased effective frequency.

4.2.1 Inductor Selection

$$D_{\max} = \frac{V_{OUT} + V_d - V_{IN(MIN)}}{V_{OUT} + V_d + V_{(ON)}}$$

$$D_{\min} = \frac{V_{OUT} + V_d - V_{IN(MAX)}}{V_{OUT} + V_d + V_{(ON)}}$$

Where V_{OUT} is the output voltage, V_d is the forward voltage drop of the output diode, and $V_{(ON)}$ is the on stage voltage of the switching MOSFET. $V_{IN(MAX)}$ is the maximum input voltage, and $V_{IN(MIN)}$ is the minimum input voltage.

The average inductor current $I_{L(avg)}$ (maximum) per phase can be calculated knowing the output current, I_{OUT}, remembering that the current per phase is one-half the total current. This is the origin of the 0.5 term in the numerator below.

$$I_{L(avg)} = \frac{0.5xI_{OUT}}{1 - D_{MAX}}$$

As a starting point assume the peak inductor current ripple per phase, ΔI_L to be a certain percentage of the average inductor current calculated in equation. A good starting value of ΔI_L is about 40% or the output current which is 20% of the individual phase current. Inductor ripple will also determine the minimum output current for continuous mode operation, so some iteration may be necessary in choosing this parameter. The peak inductor current per phase is given by:

$$I_{PEAK} = I_{L(avg)} + \frac{\Delta I_L}{2}$$

Knowing the switching frequency, f_s the required inductance value per phase can be selected using:

$$L_{(MIN)} = \frac{(V_{IN(MIN)} - V_{(ON)})xD_{MAX}}{f_s x \Delta I_L}$$

At the boundary between CCM and DCM modes of operation, the peak inductor current per phase, I_{PEAK} is the same as the peak to peak inductor current ripple per phase, ΔI_L. Therefore, the average inductor current at the boundary is given by:

$$I_{L(avg-critical)} = \frac{\Delta I_{PEAK}}{2}$$

From above equations:

$$I_{PEAK} = \frac{I_{OUT}}{1 - D_{MAX}}$$

The critical value of the inductance per phase to maintain the converter in continuous mode related to output current is given by,

$$L_{(crit)} = \frac{(V_{IN(MIN)} - V_{ON}) x D_{MAX} x (1 - D_{MAX})}{f_s x I_{OUT}}$$

Knowing the minimum load current in a particular design, L can be chosen. Obviously, there are trade-offs between minimum load current, percent ripple, and inductor size. Increasing the frequency helps in reducing inductor size.

4.2.2 Output Capacitor Selection

In a boost converter, the output capacitor must be chosen to withstand relatively high ripple current compared to an equivalent power buck regulator. The high ripple current flows through the equivalent series resistance (ESR) of the capacitor. ESR increases the capacitor temperature and increases ripple voltage. First calculate the worst case duty cycle for ripple which is usually the maximum duty cycle (refer to Fig. 4.2 for this value). Then read the y axis value or normalized rms ripple in the output capacitor from Figure 4.2 using the two phase graph.

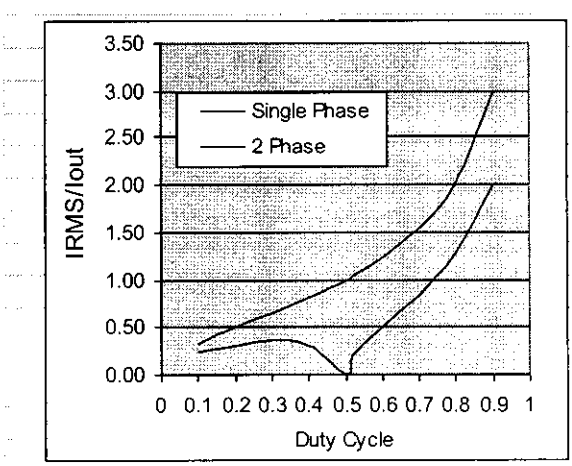

Figure 4.2 Normalized Output Capacitor Ripple Current

Then, multiply the output current by this number to get the actual RMS output capacitor ripple. Using the actual ripple, the capacitor can be selected. The capacitor must be chosen to withstand this RMS ripple current at extreme operating conditions. Frequently several capacitors in parallel can be selected. Next using the equation to determine the capacitance necessary to insure a given voltage ripple. In this case the ESR will be the dominate term which will determine the capacitor's value. Both conditions, RMS rating and ESR value must be met. In the below equation, f_s is double the frequency of an individual phase, since both phases are combined at the output capacitor.

$$\Delta_{VOUT} = \frac{I_{OUT(MAX)} x(1 - D_{MIN})}{f_s x C_{OUT}} + I_{PEAK} xESR$$

It is interesting to observe from figure the reduction in RMS (and peak to peak) ripple by using a two phase converter vs. a single phase solution. At 50% duty cycle, ripple is nearly perfectly canceled, which occurs when V_{IN} is twice V_{OUT}.

4.2.3 Input Capacitor Selection

Because an inductor is in series with the input supply in a boost converter, input capacitor selection is less severe than the output capacitor. In a two-phase design, there is a further reduction in input ripple due to ripple cancellation, allowing a smaller input capacitor than in a single phase design. The input ripple can be read from the graph in Fig. 4.3. This graph is normalized according to

$$I_{RIPPLE(Normalized)} = \frac{V_{IN}}{Lxf_s}$$

where fs is the switching frequency per phase.

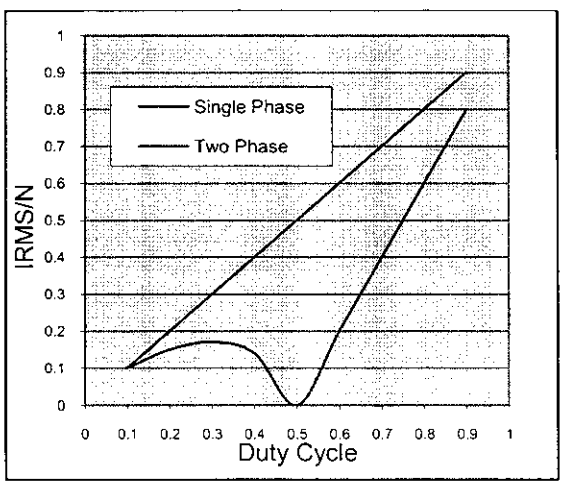

Figure 4.3 Normalized Input Capacitor Ripple Current

This normalization keeps the y axis of the graph in reasonable limits and results in an easier way to read graph. As in the output capacitor case, determine the worst case duty cycle for a given design and read the normalized ripple current from the two-phase graph. Then convert the normalized ripple current to actual ripple current by multiplying by the normalization factor. Then size the input capacitor to handle this rms ripple value.

4.2.4 Power Switches Selection

Each MOSFET should be selected based on several parameters. The drain-source breakdown should be greater than the maximum input voltage plus some margin for ringing. The $R_{DS(ON)}$ value will determine conduction losses and must low enough to keep junction temperatures within specifications at the maximum drain current condition. Gate to source and gate to drain changes will contribute to AC losses. The thermal resistance rating will determine heatsink and airflow requirements. A more detailed calculation for the power dissipated in each MOSFET is given by:

$$P_{MOSFET} = \left(\frac{I_{OUT(MAX)}}{2 \cdot (1-D)}\right)^2 \cdot R_{DS(ON)} \cdot D \cdot 1.3 + V_{IN(MAX)} \cdot Q_g \cdot f_s + \frac{0.5 \cdot V_{IN(MAX)} \cdot I_{OUT} \cdot f_s \cdot (t_R + t_F)}{1-D}$$

The first term is the I^2R term. The 1-D term in the denominator relates the output current to inductor current. The 2 in the denominator is necessary to get current per phase. The second term is the AC gate charge loss term with depends on phase frequency and the third term represents conduction switching loss.

4.2.5 Output Diode Selection

The output diode selection is based on voltage and current ratings, and reverse recovery time. The voltage rating should be V_{OUT} plus some margin for ringing. V_F should be as low as possible at the maximum output current specification to minimize conduction losses. Reverse recovery time t_{rr} should be as low as possible to minimize switching losses. Chose a Schottky rectifier if voltage ratings permit, otherwise an ultra-fast rectifier is required.

4.2.6 Compensation Components Selection

Compensation is similar to an equivalent power single phase boost regulator with the same inductor value. There is a right-half-plane zero in the continuous conduction mode which will influence loop bandwidth. A conservative approach is to insure the loop gain crosses zero at lower than $1/4^{th}$ the switching (per phase) frequency. The frequency of the right-half-plane zero is given by

$$f_{RHPZ} = \frac{R_{LOAD} \cdot (1-D)^2}{2 \cdot \Pi \cdot L} = \frac{R_{LOAD} \cdot V_{IN}^{\ 2}}{2 \cdot \Pi \cdot L \cdot V_{OUT}^{\ 2}}$$

4.3 SIMULATION DESCRIPTION

The project module is simulated using MATLAB 7.7.0(R2008b). The simulation is executed under ode23tb (stiff/TR-BDF2) state which is used to fasten the execution speed and the Zero-crossing control is disabled. The solver method is set to fast. The voltage is measured at different points in the simulation circuit. The system is tested with different load and wind speed. The designed system generates AC power with asynchronous generator (215HP; 400V; 50Hz). It utilizes a three-phase asynchronous machine model and a three-phase rectifier-inverter model based on a-b-c reference frame to simulate the performance of the generation system. The IG design is made with the calculated value of resistance, flux linkage of the stator and rotor windings and with the torque equation and the number of poles. The generated power is rectified. The generated power varies with the wind speed. The power converter converts the three phase AC to DC and then the filter circuit is used for obtaining smooth DC voltage across it. This DC voltage is then boosted with the interleaved boost converter (IBC). Theoretically IBC can boost up to 200%. The DC voltage is fed to the inverter before which it is regulated to desired voltage in a closed loop with PWM technique. Thus the output at the IBC is always constant – rated voltage. This DC voltage is then regulated AC three phase with IGBT's. An IGBT inverter is designed with a open loop PWM technique and feed the AC load. PWD signal is designed in close loop and open loop system with PID and PI controller respectively. The PWM signal is generated to regulate the DC voltage that in turn gives a fixed AC supply from the inverter. Thus a regulated Three Phase AC supply is transmitted to the Load.

Figure 4.4 shows the simulation circuit of the proposed system with boost circuit.

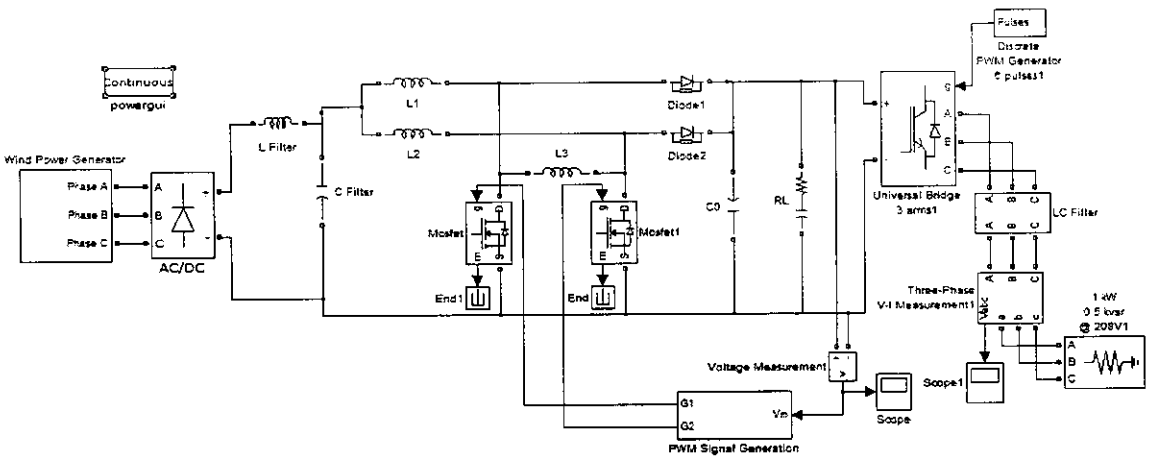

Figure 4.4 Simulation Circuit of the proposed system

Figure 4.5 shows the wind induction generator model which operates on different wind speed.

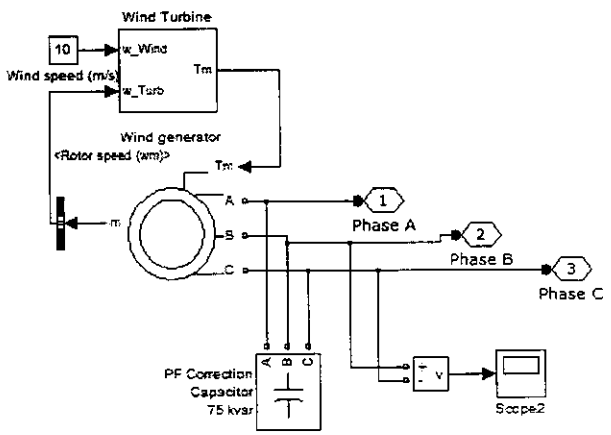

Figure 4.5 Wind Induction Generator

The open loop PWM pulse generator is shown in Figure 4.6

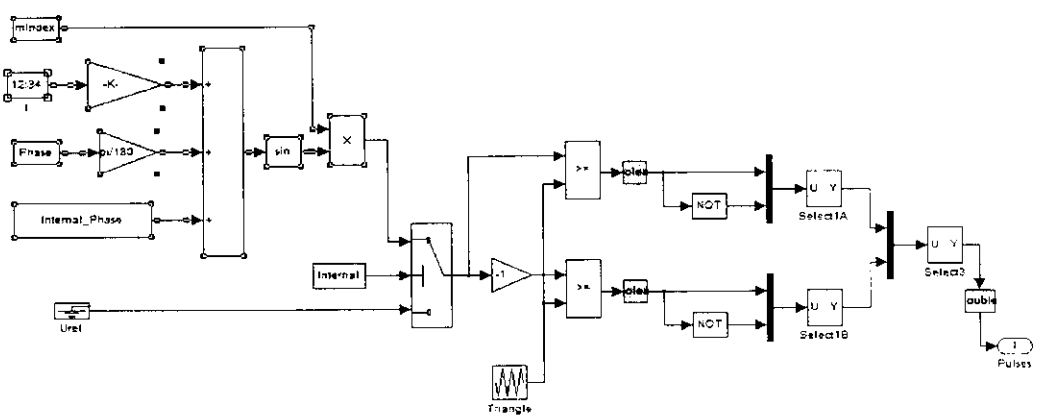

Figure 4.6 PWD signal for inverter

The control circuit of the IBC is shown in Figure 4.7 The PWM signal for the IBC is generated in this block. To reduce the ripple and noise in the inverted AC signal a 3-phase LC circuit is used.

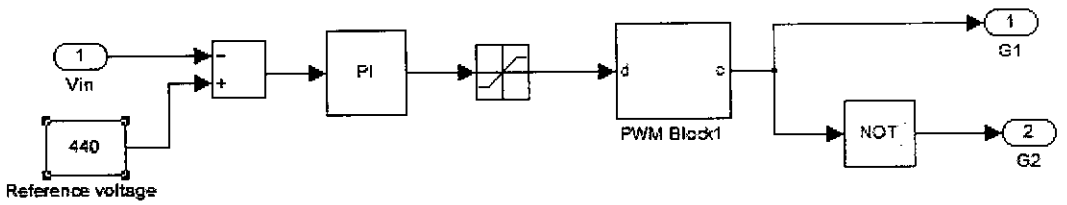

Figure 4.7 PWD Signal for IBC

4.4 RESULT DISCUSSIONS

The system is tested under different wind speed and different load conditions. The result shown here is examined when the wind speed is 7m/s and the reference voltage is set at 220V. The Figure 4.8 shows the generated voltage when wind speed is 7m/s. The voltage measured at this instant is 160V AC. Fig 4.9 shows the current wave form generated along with the generated voltage.

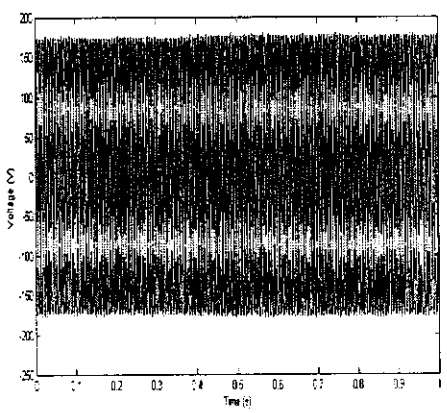

Figure 4.8 Input voltage 160V AC

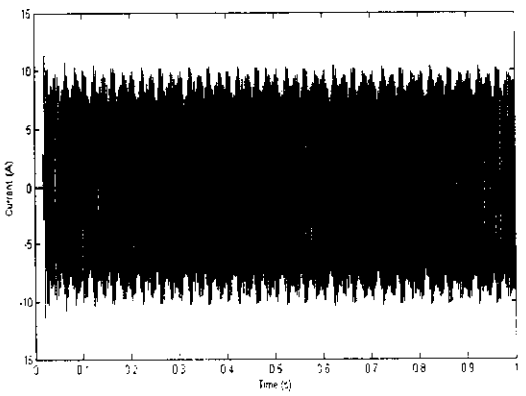

Figure 4.9 Input current 10A

Fig 4.10 shows the rectified voltage which is measured at the output of the LC filter. The rectified voltage is measured to be 160V DC. Fig 4.11 shows the IBC output which is 220V DC.

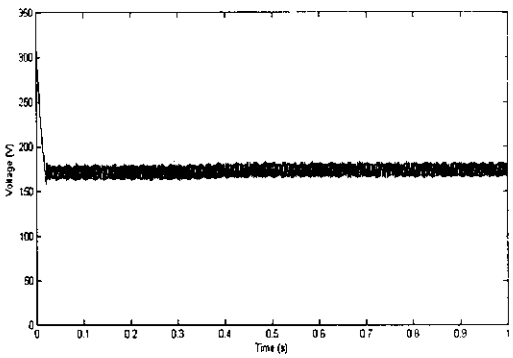

Figure 4.10 Rectified DC 160V

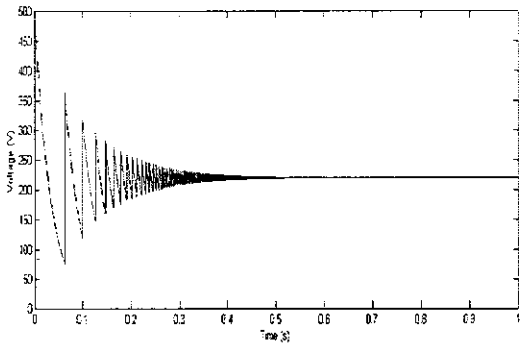

Figure 4.11 IBC controlled Output 220V DC

Figure 4.12 and 4.13 shows the inverter output with and without IBC.

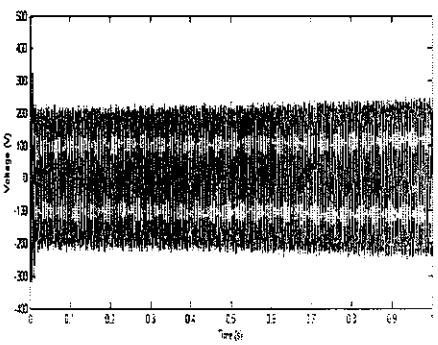

Fig 4.12 Output Voltage with IBC 220V AC

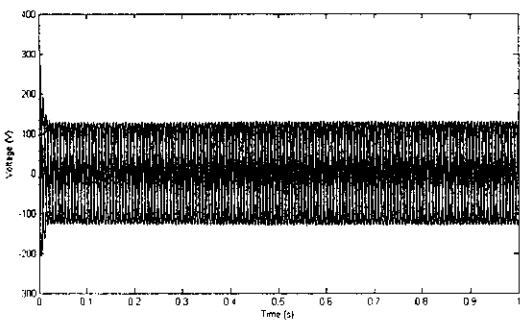

Fig 4.13 Output Voltage without IBC 120V

Figure 4.14 shows the current waveform of 3A at the load terminal.

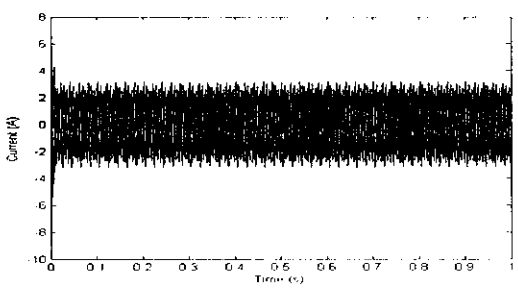

Figure 4.14 Output current 3A (IBC)

Fig 4.15 and 4.16 shows the Total Harmonic Distortion (THD) waveform for input and output voltage waveform. From the THD graph it is clear that the harmonics distortion is reduced with IBC.

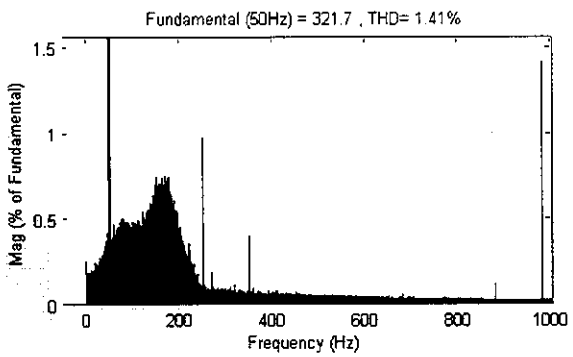

Figure 4.15 THD for output Voltage 220V AC

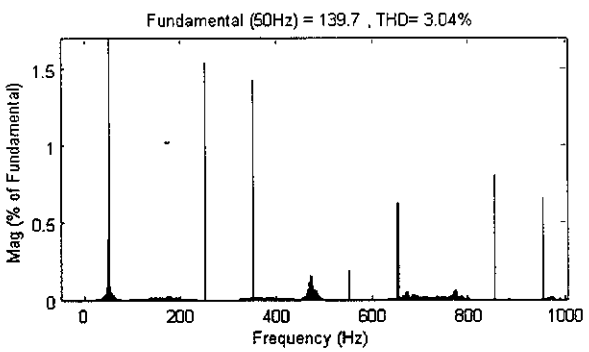

Figure 4.16 THD for input voltage 160V AC

CHAPTER 5

HARDWARE MODEL OF THE PROPOSED SYSTEM

5.1 SCHEMATIC DIAGRAM OF PROPOSED SYSTEM

The block diagram of the proposed system is shown in figure 5.1. It has fixed AC source input, a diode rectifier, IBC and inverter connected to the 3-phase load. The control part of the circuit is design with PIC microcontroller.

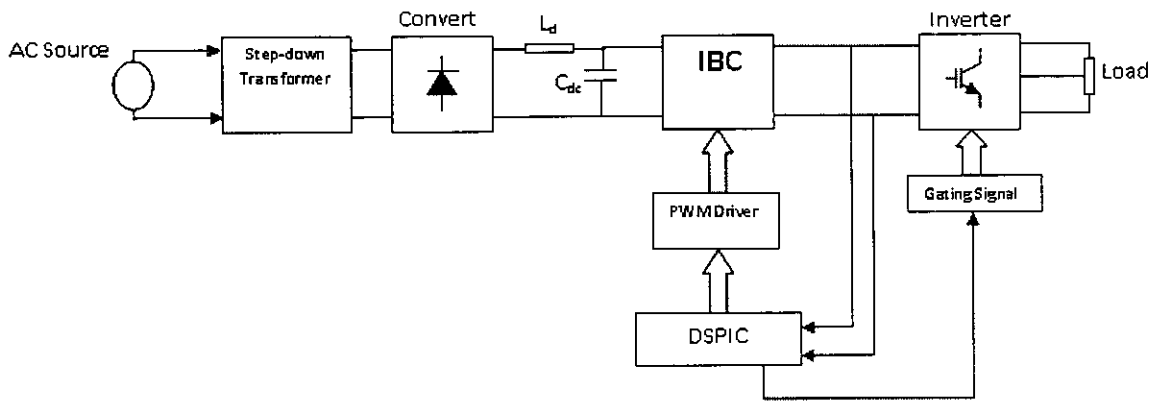

Figure 5.1 Block Diagram of Proposed System

5.2 BLOCK DIAGRAM DESCRIPTION

The entire system is divided into the following subsystems for the easiness of understanding.

- Power Supply Circuit.
- Interleaved Boost Converter.
- PIC 16f877A
- Driver circuit
- Optocoupler

The figure 5.2 shows the experimental setup used in this project. The ac supply is converted to DC voltage with diode rectifier. The rectified voltage is boosted in IBC part and it stabilized at 24V DC. The stabilization is made with the help of PWM signal generated by the PIC16F877A microcontroller. The IBC voltage is maintained constant in close loop part taking the reference voltage at the output of the output of the IBC. Driver circuits are provided through ICs IRS 2110 for the rectifier. Optocouplers are provided between the

power circuit and the signal level circuit for isolation. The switching pulses are generated by the PIC using the SPWM technique.

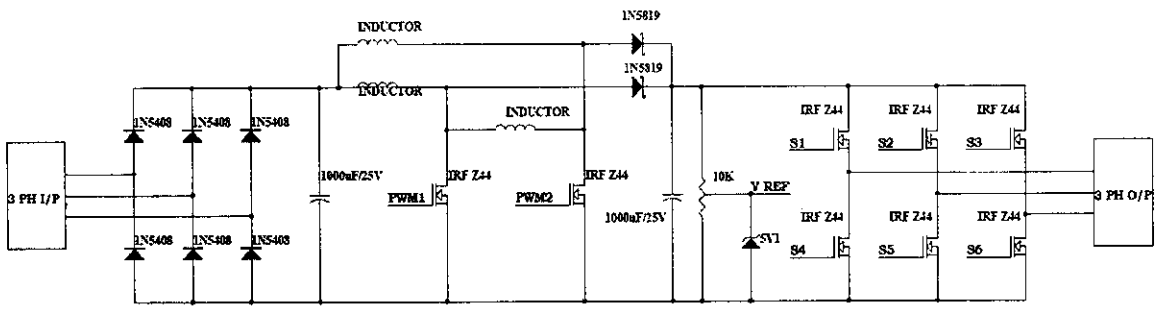

Figure 5.2 Schematic diagram of Proposed System

5.2.1 THE POWER SUPPLY UNIT

The AC voltage, typically 230V RMS, is connected to an transformer, which steps that ac voltage down to the level of the desired AC output. A diode rectifier then provides a full-wave rectified voltage that is initially filtered by a simple capacitor filter to produce a dc voltage. This resulting dc voltage usually has some ripple or ac voltage variation.

A regulator circuit removes the ripples and also remains the same dc value even if the input dc voltage varies, or the load connected to the output dc voltage changes. This voltage regulation is usually obtained using one of the popular voltage regulator IC units. The power circuit diagram is shown in figure 5.3

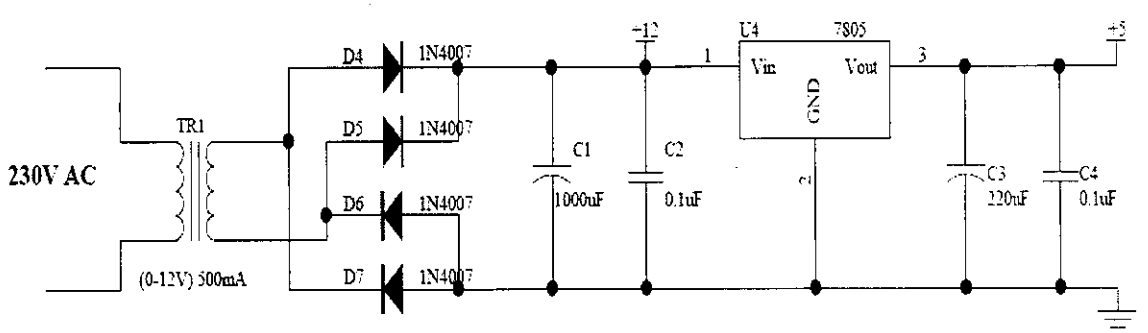

Figure 5.3 Power Supply Circuit

5.2.2 PULSE GENERATING CIRCUIT

PIC16F877A microcontroller is used as the pulse generating circuit and Driver circuit is used to remove the harmonics, buffer and filter the PWM signal. PIC16F877A is a 40 pin; CMOS flash microcontroller with A/D controller.

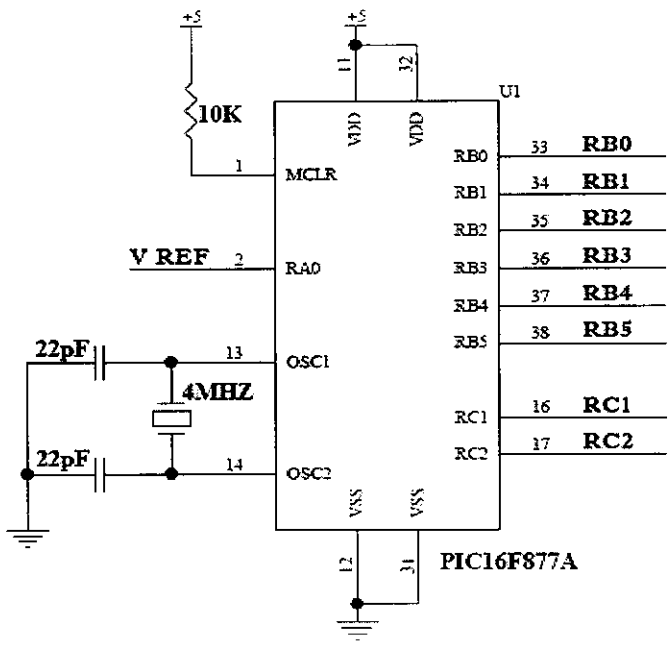

Figure 5.4 Pin configuration of PIC16F877A

High-Performance RISC CPU

- Only 35 single word instructions to learn
- All instructions are 1μs (@4MHz) except for program branches which are 2 cycles
- Operating speed: DC - 20MHz clock input.

Peripheral Features

- Two 8-bit timer/counter (TMR0, TMR2) with 8-bit programmable prescaler.
- 12.5 ns resolution for PWM mode.
- Two Capture/Compare PWM (CCP) Module.
- Brown-out detection circuitry for brown-out Reset (BOR).

Special Micro controller Features

- Power-On Reset

- Power-up Timer (PWRT) and Oscillator Start-Up Timer (OST)
- Selectable oscillator options.
- Watchdog timer (WDT) with its own on-chip RC oscillator for reliable operation.
- Self-reprogrammable under software control.
- Power saving Sleep mode.

5.2.3 DRIVER CIRCUIT

The system uses two driver circuits. One for IBC gating signal and the other driver circuit is for the inverter. The inverter requires 6-gatting pulse and that is driven PIC Port B. The signal from port B is coupled with optocoupler, the reason behind is that optocoupler can be used in high switching frequency compared to other electronic devices. The switching frequency used here is 10KHz frequency. Fig 5.5 shows the driver circuit for the 3-phase inverter. The diagram shown here represents the driver circuit for one switch. A similar arrangement of driver is connected to port B of PIC microcontroller to drive other 5 switches in the inverter.

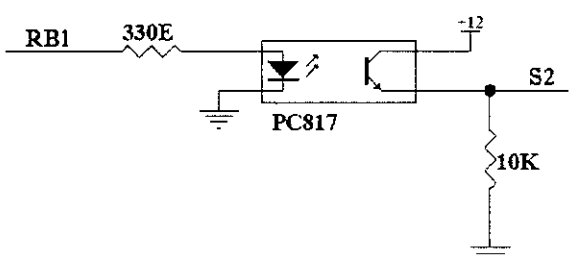

Figure 5.5 Inverter driver circuit

Optocoupler

Optocoupler is also termed as optoisolator. Optoisolator a device which contains a optical emitter, such as an LED, neon bulb, or incandescent bulb, and an optical receiving element, such as a resistor that changes resistance with variations in light intensity, or a transistor, diode, or other device that conducts differently when in the presence of light. These devices are used to isolate the control voltage from the controlled circuit.

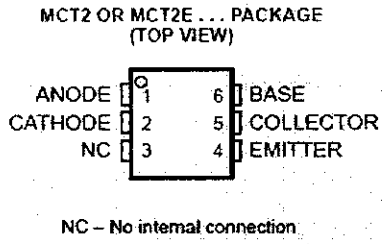

Figure 5.6 MCT2E Optocoupler

- High Direct-Current Transfer Ratio
- Base Lead Provided for Conventional Transistor Biasing
- High-Voltage Electrical Isolation . . .
- 1.5-kV, or 3.55-kV Rating
- Plastic Dual-In-Line Package
- High-Speed Switching:

IBC Driver circuit

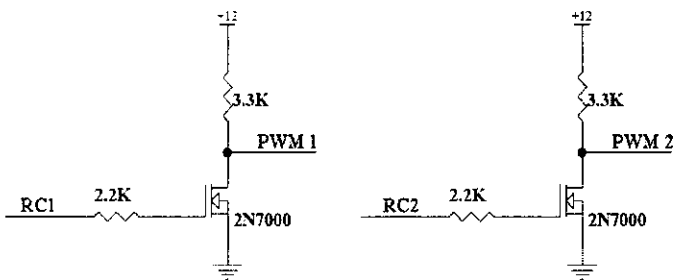

Figure 5.7 IBC Driver Circuit

The driver circuit for IBC is shown in figure 5.6. the driver circuit consist of MOSFET switched that drive the signal from PIC microcontroller to the IBC.

5.3HARDWARE TESTING AND RESULTS

The fabricated hardware model is as shown in fig.5.7. The output waveforms of the rectifier, boost and the inverter are shown in the figures 5.8, 5.9 and 5.10 respectively. An average value of 11.7 V DC is obtained in the rectifier. The rectified DC is boosted in the IBC and maintained at 24V DC. The controlled DC voltage is converted to three phase AC in the inverter and connected to load.

Figure 5.8 Hardware Photocopy

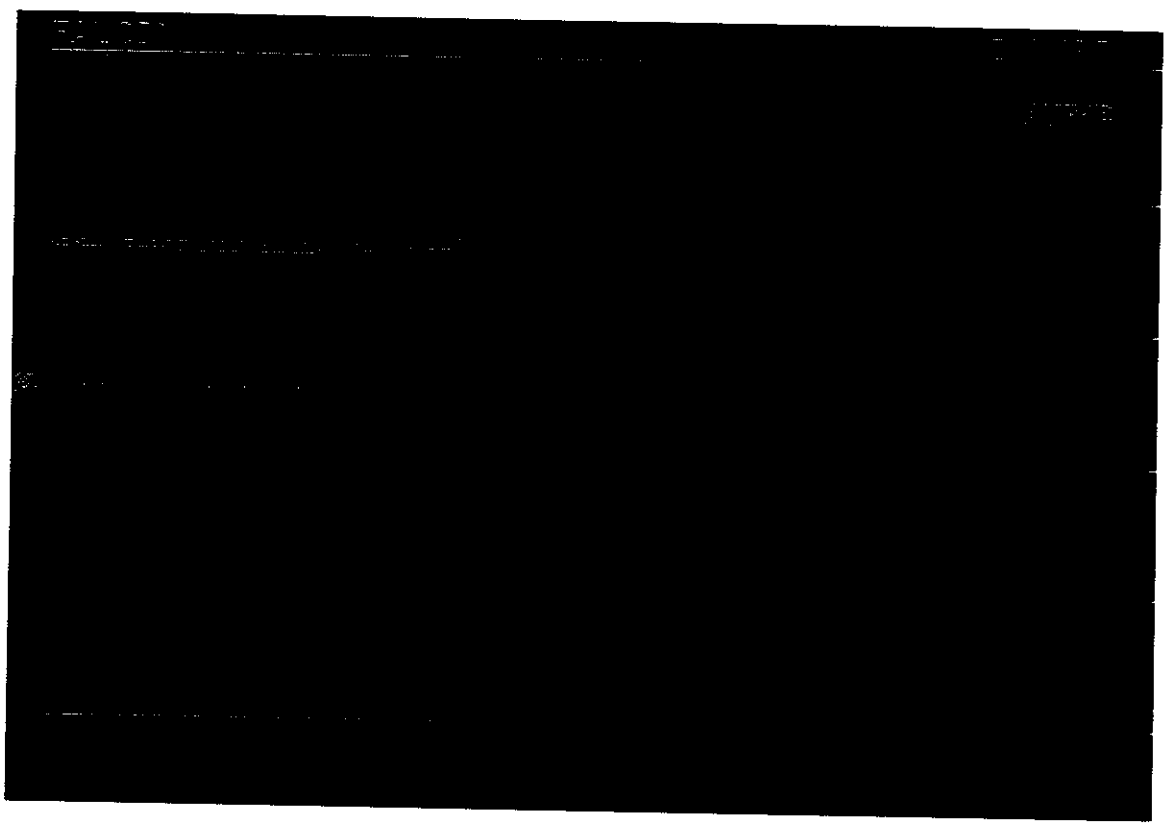

Figure 5.9 Rectifier Voltage

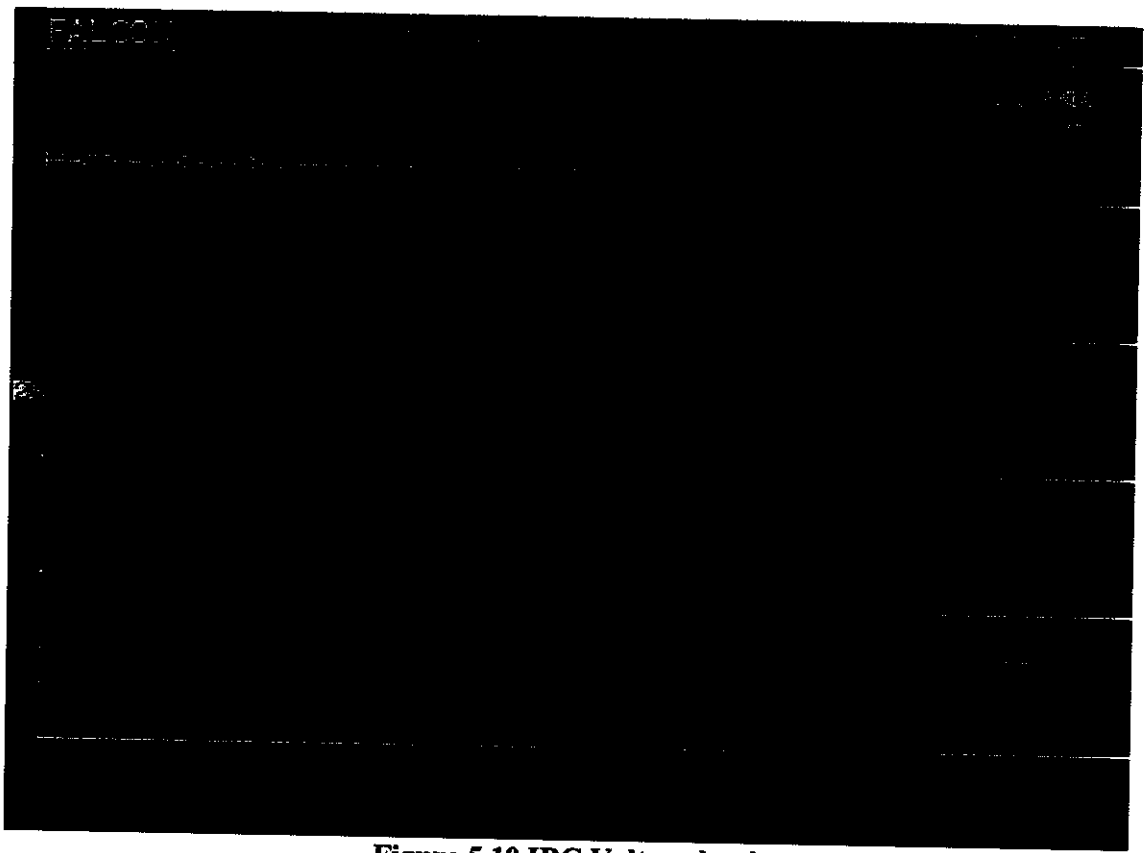

Figure 5.10 IBC Voltage level

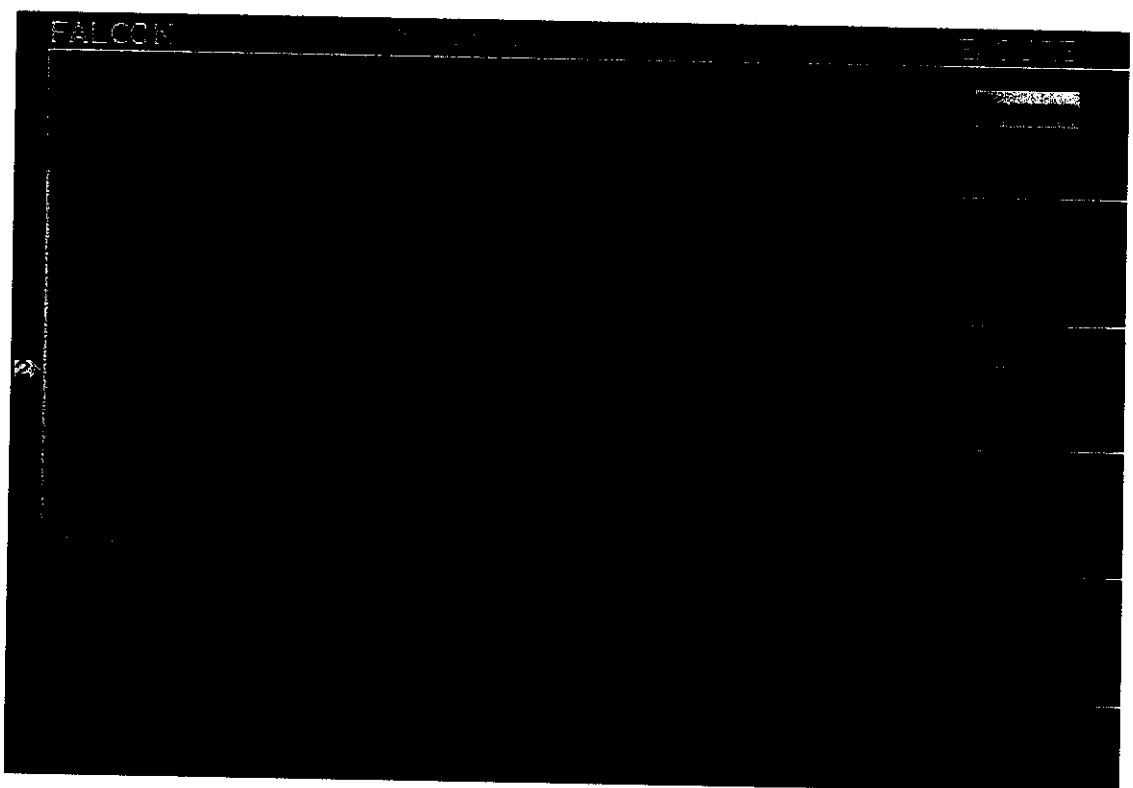

Figure 5.11 Inverter line-line Voltage CHAPTER 6

CONCLUSION AND FUTURESCOPE

Thus the designed and implemented power converter with Interleaved Boost Circuit for an autonomous three phase wind self-excited induction generator (SEIG) feeding various isolated loads is tested. From the above simulated results, it can concluded that, even at low wind speed and low power generation the required voltage can be obtained at the output. The main advantage of the system is that the minimum wind speed required for the power generation can be reduced and generator power ratings can be reduced. The gear mechanism between the turbine and the shaft can be reduced and the generator can be enabled to work in wide speed range. The displayed output is taken when the wind speed is 7m/s. At this speed the generator generates 160V AC and this voltage is boosted in the IBC to 220V DC which is the required voltage level. Steady-state results under various loads show that the designed control system for IG can maintain at desired levels. The simulated results of output voltage validate the required performance of the proposed control scheme. Thus the voltage obtained at the output is regulated with the IBC and inverter block.

Further to reduce harmonic current flowing from the SEIG, an adequate designed filter for the studied system should be installed between the output of the SEIG and the bridge rectifier.

REFERENCES

[1]. E.D. Basset and F.M. Potter, "*Capacitive excitation of induction generators*," Trans. American Institute Electrical Engineering, vol. 54, pp. 540-545,1935.

[2]. J. Arrilaga and D.B. Watson, "*Static power conversion from self-excited induction generators*," IEEE Proceedings, vol. 125, no. 8, pp. 743-746,1978.

[3]. R. Ramkumar, "*Renewable energy sources and developing countries*," IEEE Trans. Power Apparatus and Systems, vol. 102, no. 2, pp. 502-510,1983

[4]. S.S. Murthy, O.P. Malik, and A.K. Tandon, "*Analysis of self excited induction generators*," IEEE Proceedings, Part C—Generation, Transmission, and Distribution, vol. 129, no. 6, pp. 260-265,1982.

[5]. L. Shridhar, S.S. Murthy, and C.S. Jha, "*Selection of capacitors for the self regulated short shunt self excited induction generator,*" IEEE Trans.Energy Conversion, vol.10, no. 1, pp. 10-17,1995.

[6]. T.F. Chan, *"Steady-state analysis of self-excited induction generators,"* IEEE Trans. Energy Conversion, vol. 9, no. 2, pp. 288-296, 1994.

[7]. E. Bim, J. Szajner, and Y. Burian, "*Voltage compensation of an induction generator with long shunt connection*," IEEE Trans. Energy Conversion, vol.4, no.3, pp. 526-530, 1989.

[8]. L. Wang and C.-H. Lee, "*Dynamic analyses of parallel operated selfexcited induction generators feeding an induction motor load*," IEEE Trans. Energy Conversion, vol. 9, no. 2, pp. 479-485, 1999.

[9]. B. Singh, L. Shridhar, and C.S. Jha, *"Improvements in the performance of self-excited induction generator through series compensation*," IEEE Proceedings, Generation Transmission and Distribution, vol. 146, no. 6, pp. 602-608, 1999.

[10]. B. Singh and L.B. Shilpakar, "*Analysis of a novel solid state voltage regulator for a self-excited induction generators*," IEEE Proceedings,Generation Transmission and Distribution, vol. 145, no. 6, pp. 647-655,1998.

[11]. E.G. Marra and J.A. Pomilio, "*Induction-generator-based system providing regulated voltage with constant frequency,"* IEEE Trans. Industrial Electronics, vol. 47, no. 4, pp. 908-914, 2000.

[12]. E.G. Marra and J.A. Pomilio, "*Self-excited induction generator controlled by a VS-PWM bidirectional converter for rural applications*," IEEE Trans. Industry Applications, vol. 35, no. 4, pp. 877-883, 1999.

[13]. S. Wekhande and V. Agarwal, "*Simple control for a wind-driven induction generator,*" IEEE Industry Applications Magazine, vol. 7, no. 2, pp. 45-53, 1999.

[14]. R.M. Hillooala and A.M. Sharaf, "*A rule-based fuzzy logic controller for a PWM inverter in a stand alone wind energy conversion scheme*," IEEE Trans. Industry Applications, vol. 32, no. 1, pp. 57-65, 1996.

[15]. P.C. Krause, "*Analysis of Electric Machinery*", New York: McGraw-Hill Book Company, 1987.

[16]. S.-C. Kuo and L. Wang, "*Analyses of an isolated self-excited induction generator feeding a rectifier load*," IEEE Proceedings, Generation Transmission and Distribution, vol. 149, no. 1, pp. 90-97, 2002.

[17]. S.-C. Kuo and L. Wang, "*Analysis of voltage control for a self-excited induction generator using a current-controlled voltage source inverter (CC-VSI),*" IEEE Proceedings, Generation Transmission and Distribution, vol. 148, no. 3, pp. 1-8, 2001.

[18]. Oyama, J., Higuchi, T., Yamada, E., Koga, T., and Lipo, T., "*New Control Strategies for Matrix Converter*," IEEE Power Electron. Spec. Conf. Rec., pp. 360-367, 1997.

[19]. Sobczyk, T., "*Numerical Study of Control Strategies for Frequency Conversion with a Matrix Converter*," Proceedings of Conference on Power Electronics and Motion Control, Warsaw, Poland, pp. 497-502, 2000,

[20]. Cho, J.G., and Cho, G.H, "*Soft-switched Matrix Converter for High Frequency direct AC-to-AC Power Conversion*," Int. J. Electron., pp. 669-680,2007.

[21]. Zuckerberger, A., Weinstock, D., Alexandrovitz A., "*Single-phase Matrix Converter*," IEEE Proc. Electric Power App, Vol.144(4), pp. 235-240, Jul 2005

[22]. Hosseini, S.H.; Babaei, E, "*A new generalized direct matrix converter*," Industrial Electronics, 2006. Proc. ISIE 2006. Vol(2) , pp1071- 1076, 2001

[23]. Abdollah Koei & Subbaraya Yuvarajan, "*Single- Phase AC-AC Converter Using Power Mosfets*," IEEE Transaction on Industrial Electronics, Vol. 35, No.3, pp442- 443, August 2004

APPENDIX I

ARCHITECTURE OF PIC 16F877

Device	Program FLASH	Data Memory	Data EEPROM
PIC16F873	4K	192 Bytes	128 Bytes
PIC16F876	8K	368 Bytes	256 Bytes

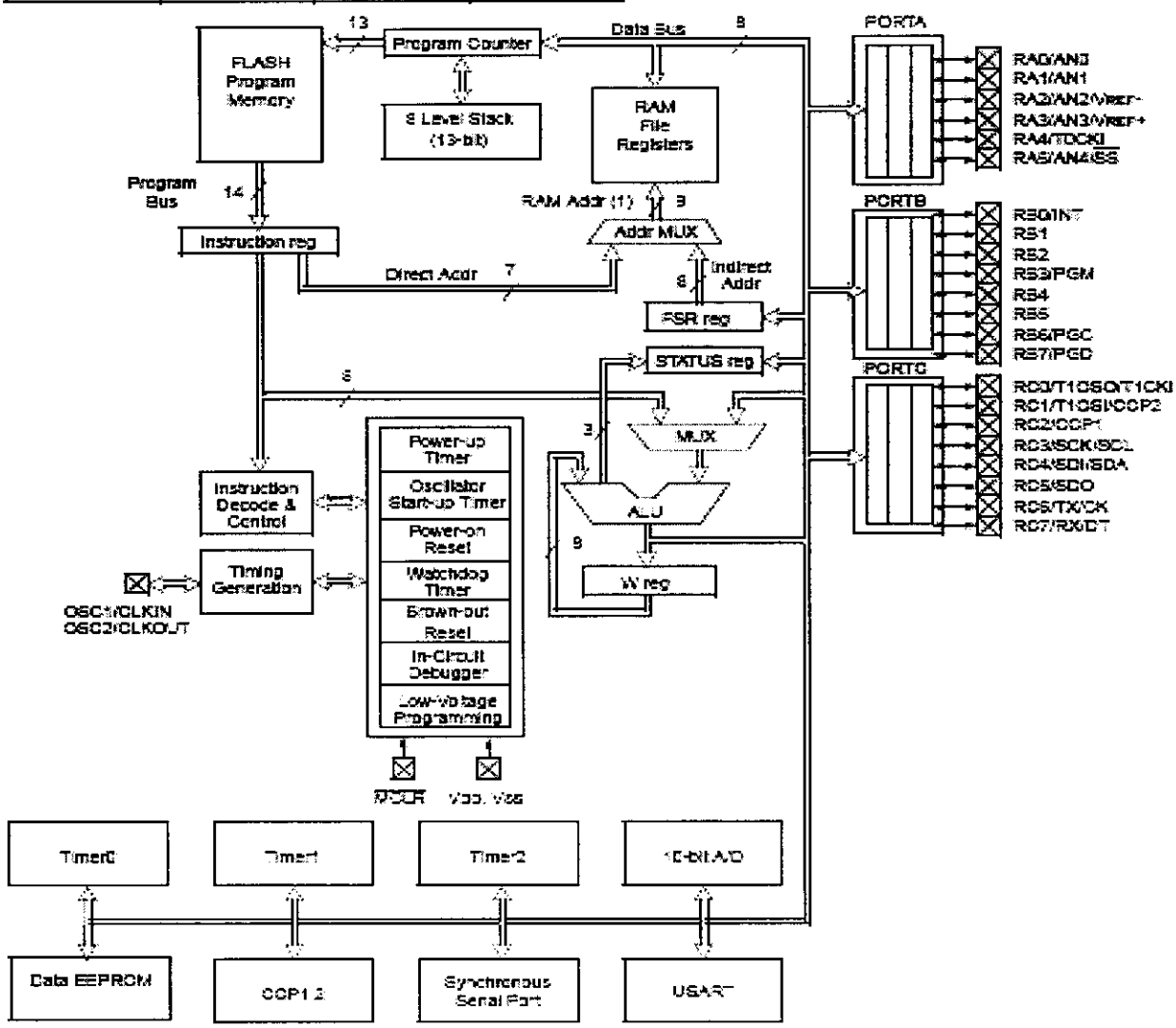

Pin Configuration Of PIC16F877A

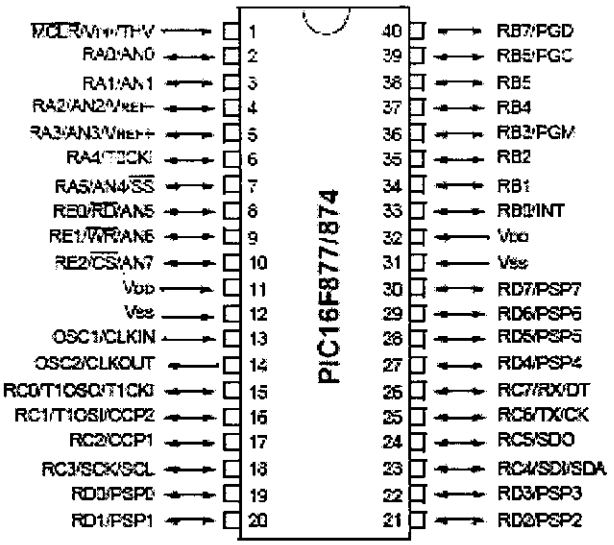

TIMERS 0 BLOCK DIAGRAM

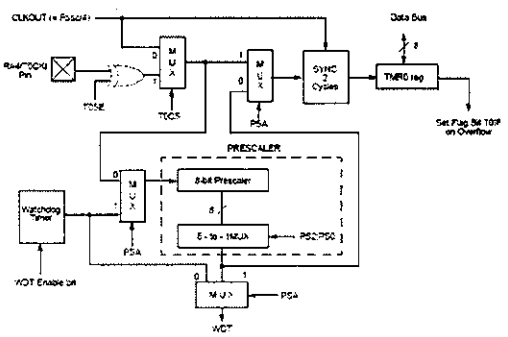

TIMER 1 BLOCK DIAGRAM

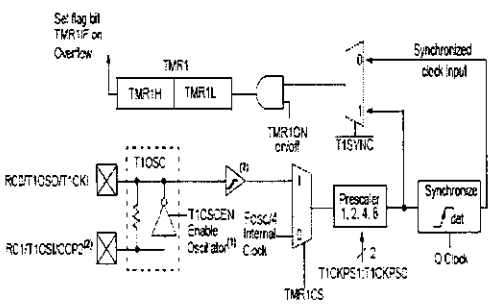

TIMER2 BLOCK DIAGRAM

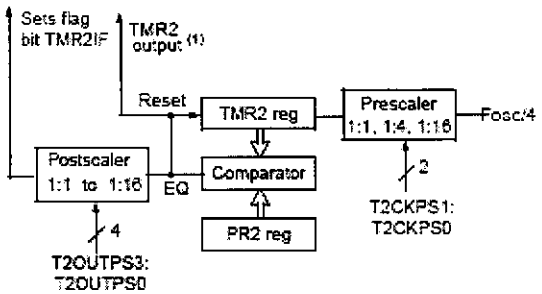

CAPTURE MODE OPERATION BLOCK DIAGRAM

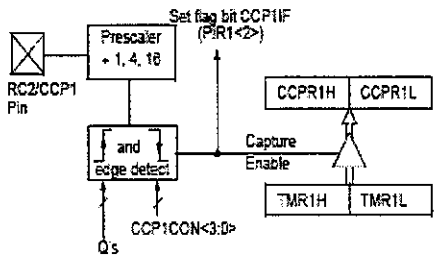

COMPARE MODE OPERATION BLOCK DIAGRAM

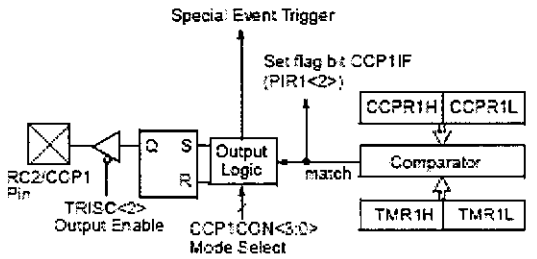

FEATURES OF PIC

- High-performance RISC CPU
- Only 35 single word instructions to learn
- Operating speed: DC - 20 MHz clock input
- DC - 200 ns instruction cycle
- Up to 8K x 14 words of Flash Program Memory,
- Up to 368 x 8 bytes of Data Memory (RAM)
- Up to 256 x 8 bytes of EEPROM data memory

- Interrupt capability (up to 14 internal/external)
- Eight level deep hardware stack
- Direct, indirect, and relative addressing modes
- Power-on Reset (POR)
- Power-up Timer (PWRT) and Oscillator Start-up Timer (OST)
- Watchdog Timer (WDT) with its own on-chip RC Oscillator for reliable operation
- Programmable code-protection
- Power saving SLEEP mode
- Selectable oscillator options
- In-Circuit Serial Programming (ICSP) via two pins
- Only single 5V source needed for programming capability
- In-Circuit Debugging via two pins
- Wide operating voltage range: 2.5V to 5.5V
- High Sink/Source Current: 25 mA
- Commercial and Industrial temperature ranges
- Low-power consumption:< 2 mA typical @ 5V, 4 MHz,20mA typical @ 3V, 32 kHz
  < 1mA typical standby current

APPENDIX II

PIC PROGRAMMING

```
#include<pic.h>
__CONFIG(0X20E4);
__CONFIG(0X3FFF);


unsigned int REFF1,INPUT1,REFF2,INPUT2;
unsigned char count;

delay(void);
delay1(void);

void main()
{
        TRISC=0;
        PORTC=0;

        TRISA=0XFF;

        ANSEL=0X0F;
        ANSELH=0;
        ADCON1=0X80;

        PR2=99;
        T2CON=0X04;


        CCP1CON=0X0F;
        CCPR1L=25;

        CCP2CON=0X0C;
```

```
        CCPR2L=75;


        while(1)
        {
/****************** ADC SCAN *****************/
                ADCON0=0X81;      // adc AN0
                delay();
                GODONE=1;
                while(GODONE);
                REFF1=(ADRESH*256)+ADRESL;


                ADCON0=0X89;      // adc AN1
                delay();
                GODONE=1;
                while(GODONE);
                REFF2=(ADRESH*256)+ADRESL;


/****************** ADC SCAN END ********************/

/******************  PWM LIMIT  ********************/

                        if(CCPR1L<30)
                                CCPR1L=30;
                        if(CCPR1L>85)
                                CCPR1L=85;

                        if(CCPR2L<30)
                                CCPR2L=30;
                        if(CCPR2L>85)
                                CCPR2L=85;
```

```
/************** OUTPUT REGULATION*****************/

                delay1();
                if(REFF1>600)
                        CCPR1L--;
                delay();
                if(REFF1<600)
                        CCPR1L++;
                delay1();

                delay1();
                if(REFF2>600)
                        CCPR2L++;
                delay();
                if(REFF2<600)
                        CCPR2L--;
                delay1();
                PORTB=0x42;

        while(TMR0<4);
        PORTB=0x52;
        while(TMR0<22);

        PORTB=0x50;
        while(TMR0<26);
        PORTB=0x30;
        while(TMR0<30);

        PORTB=0x38;
        while(TMR0<48);
        PORTB=0x28;
        while(TMR0<52);
```

```
PORTB=0x0C;
while(TMR0<56);
PORTB=0x0E;
while(TMR0<74);

PORTB=0x06;
while(TMR0<78);
TMR0=0;

PORTB=0x42;
while(TMR0<8);
PORTB=0x52;
while(TMR0<44);

PORTB=0x50;
while(TMR0<52);
PORTB=0x30;
while(TMR0<60);

PORTB=0x38;
while(TMR0<96);
PORTB=0x28;
while(TMR0<104);

PORTB=0x0C;
while(TMR0<112);
PORTB=0x0E;
while(TMR0<148);

PORTB=0x06;
while(TMR0<156);
TMR0=0;

}
```

```
}
delay()

{
        unsigned int i;
        for(i=0;i<100;i++);
}
delay1()
{
        unsigned int j;
        for(j=0;j<10000;j++);
}
```

International
IOR Rectifier

Data Sheet No. PD60147 Rev.T

IR2110(S)/IR2113(S) & (PbF)

HIGH AND LOW SIDE DRIVER

Features

- Floating channel designed for bootstrap operation
  Fully operational to +500V or +600V
  Tolerant to negative transient voltage
  dV/dt immune
- Gate drive supply range from 10 to 20V
- Undervoltage lockout for both channels
- 3.3V logic compatible
  Separate logic supply range from 3.3V to 20V
  Logic and power ground ±5V offset
- CMOS Schmitt-triggered inputs with pull-down
- Cycle by cycle edge-triggered shutdown logic
- Matched propagation delay for both channels
- Outputs in phase with inputs
- Also available LEAD-FREE

Product Summary

V_{OFFSET}	(IR2110)	500V max.
	(IR2113)	600V max.
I_O+/-		2A / 2A
V_{OUT}		10 - 20V
$t_{on/off}$ (typ.)		120 & 94 ns
Delay Matching	(IR2110)	10 ns max.
	(IR2113)	20ns max.

Packages

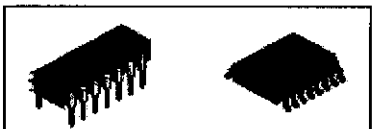

14-Lead PDIP
IR2110/IR2113

16-Lead SOIC
IR2110S/IR2113S

Description

The IR2110/IR2113 are high voltage, high speed power MOSFET and IGBT drivers with independent high and low side referenced output channels. Proprietary HVIC and latch immune CMOS technologies enable ruggedized monolithic construction. Logic inputs are compatible with standard CMOS or LSTTL output, down to 3.3V logic. The output drivers feature a high pulse current buffer stage designed for minimum driver cross-conduction. Propagation delays are matched to simplify use in high frequency applications. The floating channel can be used to drive an N-channel power MOSFET or IGBT in the high side configuration which operates up to 500 or 600 volts.

Typical Connection

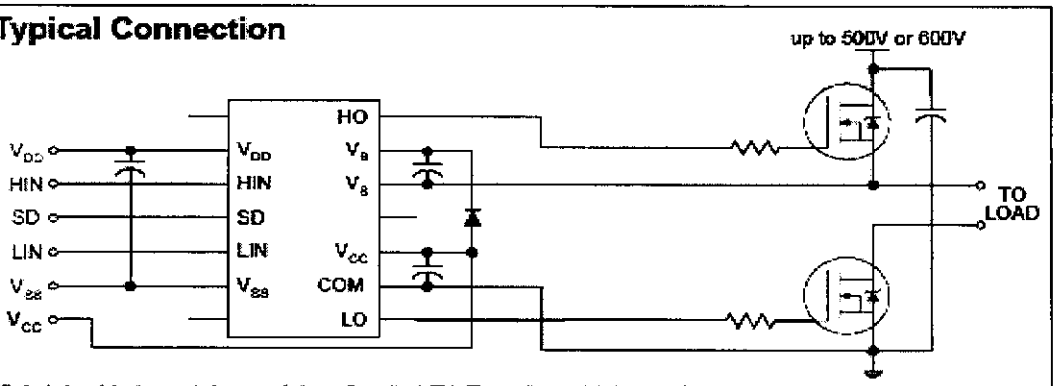

(Refer to Lead Assignments for correct pin configuration). This/These diagram(s) show electrical connections only. Please refer to our Application Notes and DesignTips for proper circuit board layout.

Absolute Maximum Ratings

Absolute maximum ratings indicate sustained limits beyond which damage to the device may occur. All voltage parameters are absolute voltages referenced to COM. The thermal resistance and power dissipation ratings are measured under board mounted and still air conditions. Additional information is shown in Figures 28 through 35.

Symbol	Definition		Min.	Max.	Units
V_B	High side floating supply voltage	(IR2110)	-0.3	525	V
		(IR2113)	-0.3	625	
V_S	High side floating supply offset voltage		V_B - 25	V_B + 0.3	
V_{HO}	High side floating output voltage		V_S - 0.3	V_B + 0.3	
V_{CC}	Low side fixed supply voltage		-0.3	25	
V_{LO}	Low side output voltage		-0.3	V_{CC} + 0.3	
V_{DD}	Logic supply voltage		-0.3	V_{SS} + 25	
V_{SS}	Logic supply offset voltage		V_{CC} - 25	V_{CC} + 0.3	
V_{IN}	Logic input voltage (HIN, LIN & SD)		V_{SS} - 0.3	V_{DD} + 0.3	
dV_S/dt	Allowable offset supply voltage transient (figure 2)		—	50	V/ns
P_D	Package power dissipation @ $T_A \leq +25°C$	(14 lead DIP)	—	1.6	W
		(16 lead SOIC)	—	1.25	
R_{THJA}	Thermal resistance, junction to ambient	(14 lead DIP)	—	75	°C/W
		(16 lead SOIC)	—	100	
T_J	Junction temperature		—	150	°C
T_S	Storage temperature		-55	150	
T_L	Lead temperature (soldering, 10 seconds)		—	300	

Recommended Operating Conditions

The input/output logic timing diagram is shown in figure 1. For proper operation the device should be used within the recommended conditions. The V_S and V_{SS} offset ratings are tested with all supplies biased at 15V differential. Typical ratings at other bias conditions are shown in figures 36 and 37.

Symbol	Definition		Min.	Max.	Units
V_B	High side floating supply absolute voltage		V_S + 10	V_S + 20	V
V_S	High side floating supply offset voltage	(IR2110)	Note 1	500	
		(IR2113)	Note 1	600	
V_{HO}	High side floating output voltage		V_S	V_B	
V_{CC}	Low side fixed supply voltage		10	20	
V_{LO}	Low side output voltage		0	V_{CC}	
V_{DD}	Logic supply voltage		V_{SS} + 3	V_{SS} + 20	
V_{SS}	Logic supply offset voltage		-5 (Note 2)	5	
V_{IN}	Logic input voltage (HIN, LIN & SD)		V_{SS}	V_{DD}	
T_A	Ambient temperature		-40	125	°C

Note 1: Logic operational for V_S of -4 to +500V. Logic state held for V_S of -4V to $-V_{BS}$. (Please refer to the Design Tip DT97-3 for more details).

Note 2: When V_{DD} < 5V, the minimum V_{SS} offset is limited to $-V_{DD}$.

FAIRCHILD
SEMICONDUCTOR

IRF840

Data Sheet January 2002

8A, 500V, 0.850 Ohm, N-Channel Power MOSFET

This N-Channel enhancement mode silicon gate power field effect transistor is an advanced power MOSFET designed, tested, and guaranteed to withstand a specified level of energy in the breakdown avalanche mode of operation. All of these power MOSFETs are designed for applications such as switching regulators, switching converters, motor drivers, relay drivers, and drivers for high power bipolar switching transistors requiring high speed and low gate drive power. These types can be operated directly from integrated circuits.

Formerly developmental type TA17425.

Ordering Information

PART NUMBER	PACKAGE	BRAND
IRF840	TO-220AB	IRF840

NOTE: When ordering, include the entire part number.

Features

- 8A, 500V
- $r_{DS(ON)} = 0.850\Omega$
- Single Pulse Avalanche Energy Rated
- SOA is Power Dissipation Limited
- Nanosecond Switching Speeds
- Linear Transfer Characteristics
- High Input Impedance
- Related Literature
  - TB334 "Guidelines for Soldering Surface Mount Components to PC Boards"

Symbol

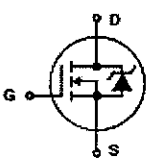

Packaging

JEDEC TO-220AB
TOP VIEW

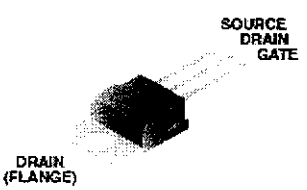

Absolute Maximum Ratings T_C = 25°C, Unless Otherwise Specified

		IRF840	UNITS
Drain to Source Voltage (Note 1)	V_{DS}	500	V
Drain to Gate Voltage (R_{GS} = 20kΩ) (Note 1)	V_{DGR}	500	V
Continuous Drain Current	I_D	8.0	A
T_C = 100°C	I_D	5.1	A
Pulsed Drain Current (Note 3)	I_{DM}	32	A
Gate to Source Voltage	V_{GS}	±20	V
Maximum Power Dissipation	P_D	125	W
Linear Derating Factor		1.0	W/°C
Single Pulse Avalanche Energy Rating (Note 4)	E_{AS}	510	mJ
Operating and Storage Temperature	T_J, T_{STG}	-55 to 150	°C
Maximum Temperature for Soldering			
Leads at 0.063in (1.6mm) from Case for 10s	T_L	300	°C
Package Body for 10s, See Techbrief 334	T_{pkg}	260	°C

CAUTION: Stresses above those listed in "Absolute Maximum Ratings" may cause permanent damage to the device. This is a stress only rating and operation of the device at these or any other conditions above those indicated in the operational sections of this specification is not implied.

NOTE:

1. T_J = 25°C to 125°C.

Electrical Specifications T_C = 25°C, Unless Otherwise Specified

PARAMETER	SYMBOL	TEST CONDITIONS		MIN	TYP	MAX	UNITS
Drain to Source Breakdown Voltage	BV_{DSS}	V_{GS} = 0V, I_D = 250µA (Figure 10)		500	-	-	V
Gate to Threshold Voltage	$V_{GS(TH)}$	V_{GS} = V_{DS}, I_D = 250µA		2.0	-	4.0	V
Zero-Gate Voltage Drain Current	I_{DSS}	V_{DS} = Rated BV_{DSS}, V_{GS} = 0V		-	-	25	µA
		V_{DS} = 0.8 x Rated BV_{DSS}, V_{GS} = 0V, T_J = 125°C		-	-	250	µA
On-State Drain Current (Note 2)	$I_{D(ON)}$	V_{DS} > $I_{D(ON)}$ x $r_{DS(ON)MAX}$, V_{GS} = 10V		8.0	-	-	A
Gate to Source Leakage Current	I_{GSS}	V_{GS} = ±20V		-	-	±100	nA
Drain to Source On Resistance (Note 2)	$r_{DS(ON)}$	V_{GS} = 10V, I_D = 4.4A (Figures 8, 9)		-	0.5	0.85	Ω
Forward Transconductance (Note 2)	g_{fs}	V_{DS} ≥ 50V, I_D = 4.4A (Figure 12)		4.0	7.4	-	S
Turn-On Delay Time	$t_{d(ON)}$	V_{DD} = 250V, I_D = 8A, R_G = 9.1Ω, R_L = 30Ω MOSFET Switching Times are Essentially Independent of Operating Temperature.		-	13	21	ns
Rise Time	t_r			-	21	35	ns
Turn-Off Delay Time	$t_{d(OFF)}$			-	50	74	ns
Fall Time	t_f			-	20	30	ns
Total Gate Charge (Gate to Source + Gate to Drain)	$Q_{g(TOT)}$	V_{GS} = 10V, I_D = 8A, V_{DS} = 0.8 x Rated BV_{DSS} ($I_{G(REF)}$ = 1.5mA (Figure 14) Gate Charge is Essentially Independent of Operating Temperature		-	42	63	nC
Gate to Source Charge	Q_{gs}			-	7.0	-	nC
Gate to Drain "Miller" Charge	Q_{gd}			-	22	-	nC
Input Capacitance	C_{ISS}	V_{GS} = 0V, V_{DS} = 25V, f = 1.0MHz (Figure 11)		-	1225	-	pF
Output Capacitance	C_{OSS}			-	200	-	pF
Reverse Transfer Capacitance	C_{RSS}			-	65	-	pF
Internal Drain Inductance	L_D	Measured from the Contact Screw on Tab to Center of Die	Modified MOSFET Symbol Showing the Internal Devices Inductances	-	3.5	-	nH
		Measured from the Drain Lead, 6mm (0.25in) from Package to Center of Die		-	4.5	-	nH
Internal Source Inductance	L_S	Measured from the Source Lead, 6mm (0.25in) from Header to Source Bonding Pac		-	7.5	-	nH
Thermal Resistance Junction to Case	$R_{\theta JC}$			-	-	1.0	°C/W
Thermal Resistance Junction to Ambient	$R_{\theta JA}$	Free Air Operation		-	-	62.5	°C/W